Published online July 2, 2018

Special Section: Hydrological Observatories

Core Ideas

- We provide an overview of the TERENO-Rur hydrological observatory.
- We present information on general physical characteristics of the Rur catchment.
- Ongoing interdisciplinary research aims to advance understanding of complex hydrological processes.

The TERENO-Rur Hydrological Observatory: A Multiscale Multi-Compartment Research Platform for the Advancement of Hydrological Science

H.R. Bogena,* C. Montzka, J.A. Huisman, A. Graf, M. Schmidt, M. Stockinger, C. von Hebel, H.J. Hendricks-Franssen, J. van der Kruk, W. Tappe, A. Lücke, R. Baatz, R. Bol, J. Groh, T. Pütz, J. Jakobi, R. Kunkel, J. Sorg, and H. Vereecken

We provide an overview of the Rur hydrological observatory, which is the main observational platform of the TERENO (TERrestrial ENvironmental Observatories) Eifel/Lower Rhine Valley Observatory. The Rur catchment area exhibits distinct gradients in altitude, climate, land use, soil properties, and geology. The Eifel National Park is situated in the southern part of the Rur catchment and serves as a reference site for the hydrological observatory. We present information on general physical characteristics of the Rur catchment and describe the main features of the multi-scale and multi-compartment monitoring framework. In addition, we also present some examples of the ongoing interdisciplinary research that aims to advance the understanding of complex hydrological processes and interactions within the Rur catchment.

Abbreviations: CRNS, cosmic-ray neutron stations; DOC, dissolved organic carbon; DOI, depth of investigation; DTN, dissolved total nitrogen; EC, eddy covariance; ECa, apparent electrical conductivity; EMI, electromagnetic induction; GPR, ground-penetrating radar; SAC_{254}, spectral absorption coefficient at 254 nm.

H.R. Bogena, C. Montzka, J.A. Huisman, A. Graf, M. Schmidt, M. Stockinger, C. Von Hebel, H.J. Hendricks-Franssen, J. Van der Kruk, W. Tappe, A. Lücke, R. Baatz, R. Bol, J. Groh, T. Pütz, J. Jakobi, R. Kunkel, J. Sorg, and H. Vereecken, Agrosphere Institute (IBG-3), Forschungszentrum Jülich, 52425 Jülich, Germany; J. Groh, Research Area 1 Landscape Functioning, Working Group Hydropedology, Leibniz Centre for Agricultural Landscape Research (ZALF), Müncheberg, Germany. *Corresponding author (h.bogena@fz-juelich.de).

Received 27 Mar. 2018.
Accepted 30 Apr. 2018.

Citation: Bogena, H.R., C. Montzka, J.A. Huisman, A. Graf, M. Schmidt, M. Stockinger, C. von Hebel, H.J. Hendricks-Franssen, J. van der Kruk, W. Tappe, A. Lücke, R. Baatz, R. Bol, J. Groh, T. Pütz, J. Jakobi, R. Kunkel, J. Sorg, and H. Vereecken. 2018. The TERENO-Rur Hydrological Observatory: A multiscale multi-compartment research platform for the advancement of hydrological science. Vadose Zone J. 17:180055. doi:10.2136/vzj2018.03.0055

Most freshwater systems are affected by human activities and require appropriate management and conservation strategies (Vörösmarty et al., 2010). Thus, predictions of the hydrological and biogeochemical cycles in response to climate change and human interventions are needed at management-relevant scales (Krause et al., 2013; Vereecken et al., 2015). This is challenging because hydrological and biogeochemical processes occur at various scales, and both natural and anthropogenic drivers need to be identified (Basu et al., 2011). The hydrological research community has to face this scientific challenge through a comprehensive consideration of multi-compartment interactions and scale dependencies to enable prediction of the response of hydrological systems to changing environmental conditions such as land use and climate change (Burt et al., 2008; Katul et al., 2012). Therefore, the development of catchment models has been a strong motivation of hydrologists (Clark et al., 2015; Ehret et al., 2014) and remains challenging where gaps in our understanding and model capability are limited by computational challenges (Clark et al., 2017). Combining state-of-the-art monitoring methods with advanced modeling techniques provides new opportunities to gain a more detailed understanding of catchment processes. In addition, such a combination would help to quantify and predict water and matter fluxes at the catchment scale and their feedback with changes in climate, land use, and water usage (Simmer et al., 2015). Such activities are still all too often constrained by a lack of long-term integrated hydrological data and missing understanding of the highly dynamic and complex hydrological processes.

To adequately characterize catchment-scale hydrological processes, an adaptive and multiscale integrated monitoring combined with dedicated experimentation and modeling activities is needed (Bogena et al., 2018). Long-term hydrological data needs to be complemented by geophysical and remote sensing measurements, providing spatial and

temporal patterns of catchment properties and states (Robinson et al., 2008; Bogena et al., 2015a). In the framework of the Terrestrial Environmental Observatories (TERENO) initiative (Zacharias et al., 2011; Bogena et al., 2012), a network of integrated observation platforms has been established in Germany with the goal to investigate the consequences of global change on the terrestrial system by (i) providing long-term data series (>15 yr) of system states and fluxes for the analysis and prognosis of climate and land use change consequences and (ii) developing and applying integrated model systems to derive more efficient prevention, mitigation, and adaptation strategies.

Within the TERENO Eifel/Lower Rhine Valley terrestrial observatory, the Rur catchment was identified as a central hydrological research area because it covers the distinct gradients in landscape features in this region. From the northern to the southern part of the observatory, altitude increases from 64 to 630 m, mean annual air temperature decreases from 10 to 7°C, and mean annual precipitation increases from 650 to 1300 mm. Along these gradients, intensively instrumented test sites have been set up to investigate specific aspects of the terrestrial system. The Eifel National Park, situated in the southern part of the Rur catchment, serves as a relatively undisturbed reference site compared with the strongly anthropogenically influenced northern part of the catchment.

Here we present a detailed overview of the integrated monitoring concept that has been established in the Rur hydrological observatory. Scientific activities with no or little reference to hydrology, which are also an important part of the TERENO concept (e.g., Zacharias et al., 2011; Bogena et al., 2012) are not treated in depth here.

Science Questions

Hydrology is a science founded on observation. Observations play an important role in the development of hydrologic theories because it is by observing changes with time, comparing observations between sites, and testing model predictions against observations that hydrologists develop an understanding of hydrological processes and responses (e.g., Burt et al., 2002). One of the key research questions addressed at the Rur hydrological observatory is: How are complex patterns of state variables and parameters of the hydrological system reflected in the heterogeneous inter- and intra-compartmental fluxes of heat energy, water, C, N, and momentum at different spatiotemporal scales? This research question is jointly studied with the collaborative Research Centre TR-32 (Simmer et al., 2015). More specific hydrological research questions that are being tackled are:

- How do patterns of soil moisture impact hydrological processes such as runoff, evapotranspiration, and water storage (e.g., Graf et al., 2014; Wiekenkamp et al., 2016b)?
- What are the key drivers for biogeochemical processes, e.g., related to nutrient transport in stream and groundwater (e.g., Wu et al., 2017; Weigand et al., 2017) and greenhouse gas emission (e.g., Gottselig et al., 2017; Liu et al., 2016; Klosterhalfen et al., 2017; Wang et al., 2018)?
- What are the key controls on travel time distributions (e.g., Stockinger et al., 2014, 2017)?
- What is the information content of spatially and temporally highly resolved soil moisture data (e.g., Korres et al., 2015; Baatz et al., 2017)?
- How do patterns in crop development and yield relate to soil water dynamics under drought conditions (e.g., Rudolph et al., 2015; Jakobi, 2017)?
- How can data assimilation and cloud computing support the real-time management of water resources (e.g., Kurtz et al., 2017)?

To answer these questions, we established a multiscale multitemporal hydrological observational platform, which is described in detail below. In addition, dedicated field campaigns and long-term experiments have been incorporated, which are also described below. We then present the data management and policy used for the Rur hydrological observatory. Finally, example key findings of the ongoing interdisciplinary research work aiming to advance the understanding of complex hydrological processes and interactions in the Rur catchment are presented.

Catchment Characteristics

The Rur catchment covers an area of 2354 km^2 and is situated mostly in North Rhine-Westphalia (Germany), but small parts belong to Belgium (157 km^2 or 6.7%) and the Netherlands (108 km^2 or 4.6%). The elevation of the terrain generally declines from south to north from 680 to 30 m asl (Fig. 1a). A detailed description of the Rur catchment with respect to land use as well as climatological, pedological, and geological characteristics is given in the following.

Land Use

More than one third of the Rur catchment area (37%) is covered by arable land (Bogena et al., 2005a), which is mainly located in the lowland regions in the northern part of the Rur catchment (Fig. 1b). This area is part of the Belgium–Germany loess belt, where crops are grown on a virtually flat terrain. The main crops are winter cereals (especially winter wheat [*Triticum aestivum* L.]), sugarbeet (*Beta vulgaris* L.), and maize (*Zea mays* L.) (Korres et al., 2015; Reichenau et al., 2016). Deciduous and coniferous forests cover a total area of 807 km^2 in the Rur catchment (34%) and are predominantly located in the upland regions. Pastures account for 22% of the land cover and are also mainly located in the upland areas. Only about 5% of the area is covered by settlements, which are mainly located in the northern part of the catchment. Remaining important land covers are open-cast lignite mines, e.g., Inden with an area of 1370 ha in 2003, and several water reservoirs located in the upland areas.

Geology

About 47% of the Rur catchment is composed of Paleozoic to Mesozoic solid rocks of the Rhenish Massif, which occur

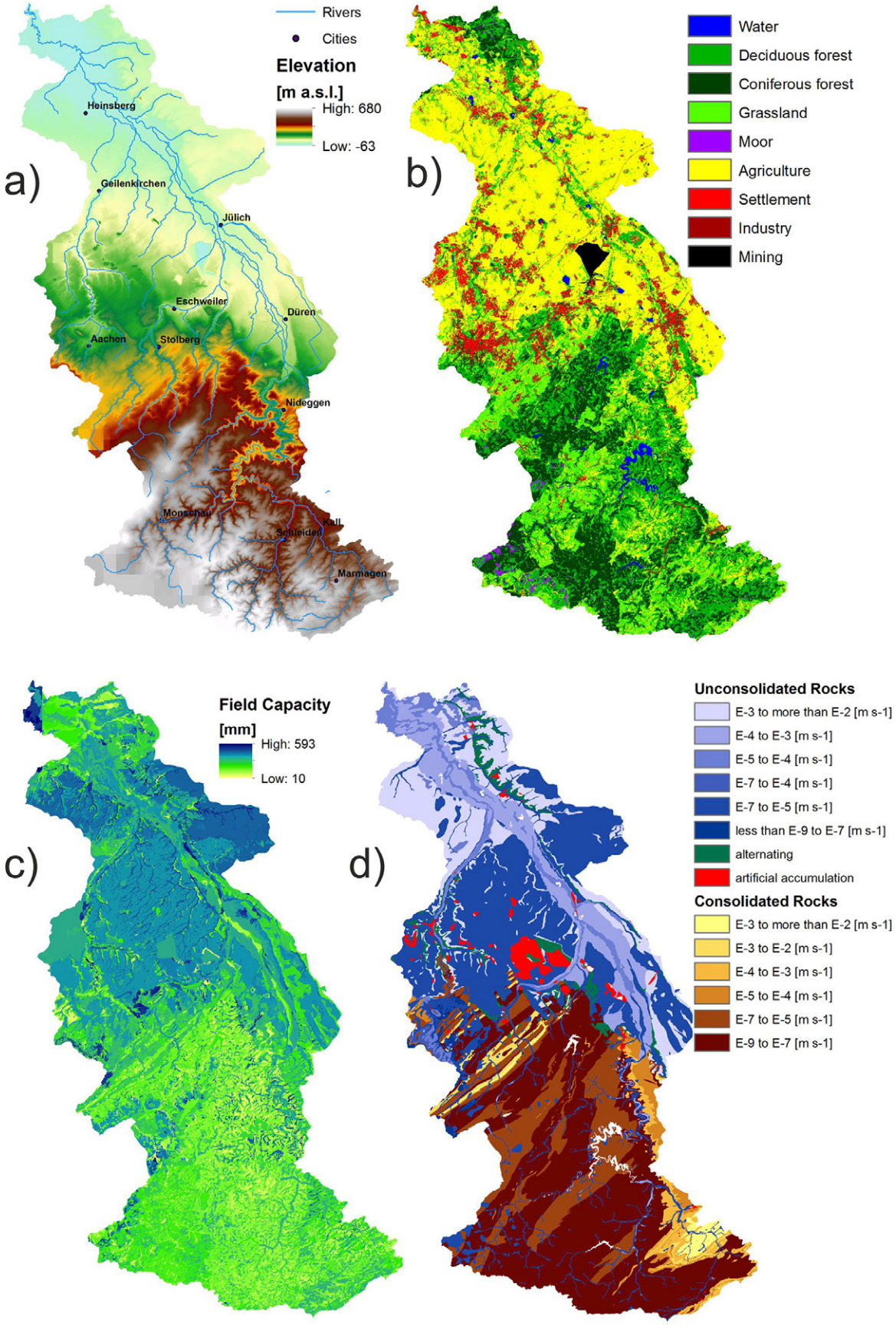

Fig. 1. Main characteristics of the Rur catchment: (a) elevation, (b) land use, (c) soil field capacity, and (d) hydrogeology (the value ranges indicate predominant saturated hydraulic conductivity). Data sources: District Council Cologne (topography), CORINE Land Cover (CLC2006); Geological Survey North-Rhine Westphalia (geology and soil).

mainly in the southern part of the Rur catchment (Bogena et al., 2005a; Fig. 1d, consolidated rocks). The Rhenish Massif mainly consists of alternating sequences of silt- and mudstones as well as sandstones and greywackes with small cavity and groundwater storage volumes. Water flow in these rocks is primarily linked to tectonic faults and jointing (Bogena et al., 2005a). Pre-Devonian solid rocks outcrop only in the High Fens Mountains in the southwestern part of the catchment and cover about 7% of the Rur catchment. Paleozoic solid rocks formed in the course of Variscan orogenesis occupy the largest area (33%). Mesozoic solid rocks (mainly semisolid sandstones superimposed by limestones) outcrop near the eastern border of the Rur catchment. Around 53% of the Rur catchment is covered by unconsolidated Tertiary and Quaternary sediments, mainly in the northern part of the Rur catchment (Fig. 1d, unconsolidated rocks). Tertiary sediments are mostly covered by Pleistocene terrace deposits (sands and gravels of the main, middle, and lower terraces of the Maas and Rur rivers) and by aeolian deposits (loess and dune sands).

Hydrogeology

The upland region is characterized by solid rock strata of low permeability and low groundwater recharge (Fig. 1d, consolidated rocks). Consequently, the water resources in this part of the Rur catchment are managed by reservoirs, which are used for drinking water supply, energy generation, and flood control. Accordingly, the upper Rur catchment shows strong seasonality, with strong runoff response after rainfall events (Rudi et al., 2010), whereas the runoff in the lower Rur catchment is strongly regulated by water management (Bogena et al., 2005a). In the adjacent flatland region to the north, abundant loose rock aquifers (Fig. 1d, unconsolidated rocks) with relatively high groundwater recharge rates exist (Bogena et al., 2005b). Accordingly, these aquifers are subject to intensive groundwater withdrawal for drinking and service water purposes. Additionally, the hydrogeology is strongly impacted by the water management required to keep the deep open-cast lignite mines free of water.

Soil

The Rur catchment can be subdivided into two major soil-landscape units. In the southern part, the major soils are Fluvisols, Gleysols (along the Rur and its tributaries), Eutric Cambisols, and Stagnic Gleysols with a silt loam texture (Fig. 1c). In the northern part, the major soils are Cumulic Anthrosols near the drainage lines and Haplic Luvisols, both with silt loam textures (Korres et al., 2015). Soils with a loamy sand texture (Fimic Anthrosols and Dystric Cambisols) are located in the northernmost part of the loess plain. The soils in the northern part are highly productive, with a mean available field capacity of >200 mm (Bogena et al., 2005a; Fig. 1c). Significantly lower available field capacities are found in the upland regions in the southern part of the Rur catchment. Here, the field capacity ranges between 50 and 150 mm and can locally fall below 30 mm.

Climate

In the northern part of the Rur catchment, the annual precipitation ranges between 650 mm/yr in the most northern part to 900 mm/yr (Bogena et al., 2005a). In the southern part of the Rur catchment, moist marine air predominantly flowing from southwest to northeast causes a significant precipitation shadowing effect. The crestal regions of the Rhenish Massif (High Fen Mountains) in the southwest receive a mean annual precipitation of 1200 mm/yr, whereas leeward precipitation levels below 700 mm/yr occur in the southeastern part of the Rur catchment. In the upland area, precipitation mainly occurs in winter when evapotranspiration rates are lowest (Bogena et al., 2005a). Due to the low evapotranspiration rates in winter and the associated high soil moisture content, a large portion of the precipitation can rapidly become runoff. In contrast, in the northern part of the Rur catchment the highest precipitation occurs in summer, with high potential evapotranspiration rates; thus, a more effective buffering of precipitation events can be assumed (Bogena et al., 2005a).

Basic Observations

The general observation strategy follows a nested multiscale approach, with sparse observations across the Rur catchment to cover the large scale (Fig. 2), moderate instrumentation at the Critical Zone Observatories Ellebach, Kall, and Erkensruhr to cover the medium scale (Fig. 2), and intense instrumentation at the small scale at the sites Selhausen (Fig. 3), Rollesbroich (Fig. 4), and Wüstebach (Fig. 5). In the following, we present the basic observations that provide necessary data for data and modeling analysis at the scale of the full hydrological observatory.

Network of Climate Stations

Key meteorological parameters including precipitation, air temperature and humidity, pressure, global radiation, wind speed, and wind direction have been recorded by a network of 12 climate stations across the Rur catchment since 2011 (Fig. 2). The stations are additionally equipped for monitoring soil temperature and soil moisture at the 10-, 20-, and 50-cm depths. The general setup of each station consists of a multiparameter weather sensor (WXT520, Vaisala), partially supplemented by a standard Hellmann type tipping bucket rain gauge (Ecotech GmbH) or a weighing rain gauge (Pluvio^2, Ott Hydromet GmbH), a pyronometer (CMP3, Kipp & Zonen), and a set of nine soil moisture sensors (HydraProbe, Stevens Water Monitoring Systems). All measurements are taken with a sampling rate of 1 Hz and stored as averages or sums in intervals of 10 min by a datalogger (Ecotech GmbH).

Network of Eddy Covariance Stations

Fluxes of sensible heat, evapotranspiration, CO_2, and momentum along with ancillary meteorological and soil variables are continuously monitored by six fixed eddy covariance (EC) stations (Fig. 2) in Selhausen, Merzenhausen, Ruraue, Rollesbroich, and in the Wüstebach catchment (forest and clear-cut area). Measurement heights of the EC instruments range between 2.0 and 37 m,

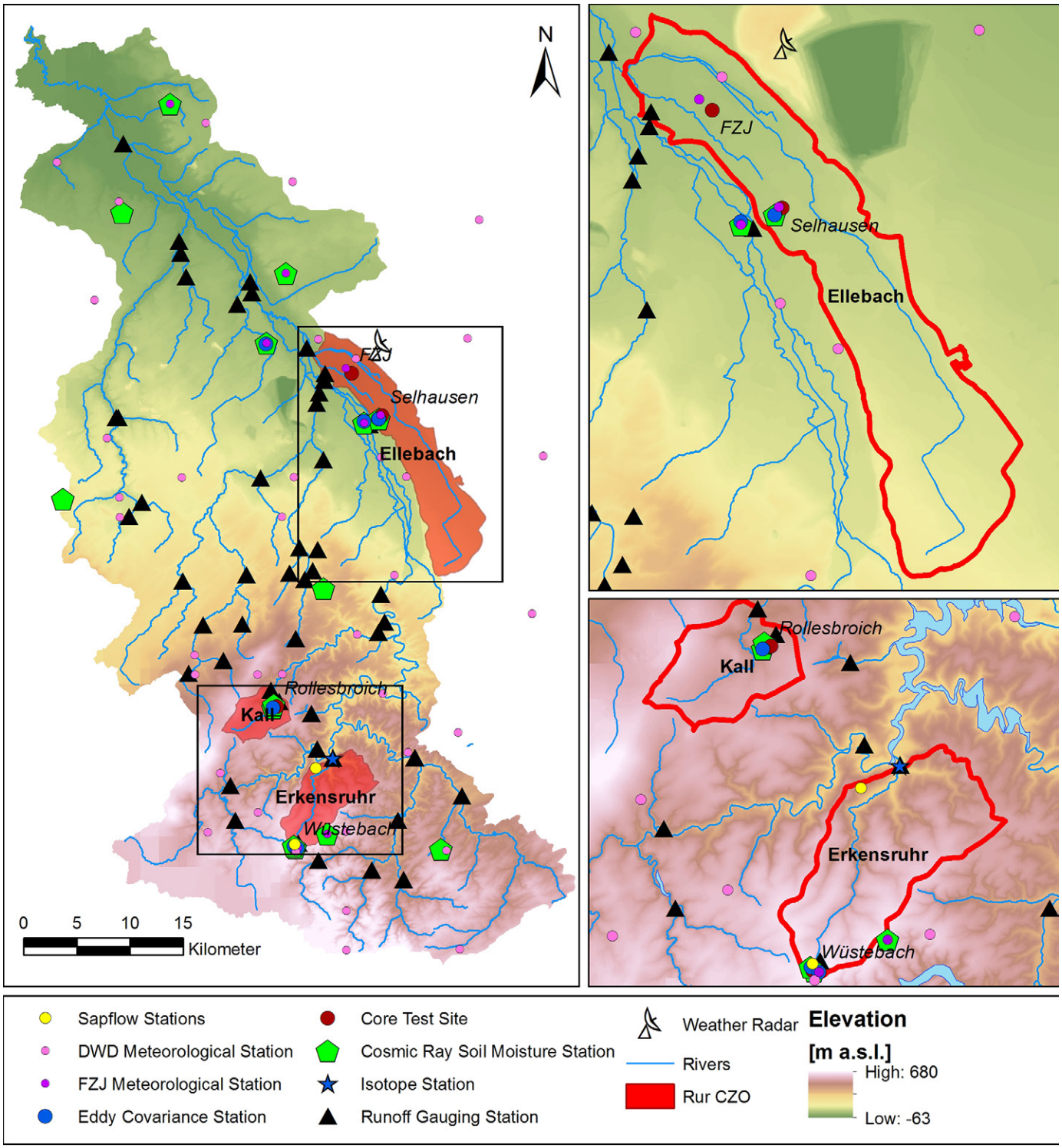

Fig. 2. The nested catchment approach and the instrumentation of the Rur hydrological observatory. Data source: District Council Cologne.

depending on the expected maximum height of vegetation at a respective site. In the forested part of the Wüstebach catchment, EC instruments are installed on the top platform of a meteorological tower at 37 m (about 12 m above the forest canopy). The common EC station setup consists of a sonic anemometer (CSAT3, Campbell Scientific) for measurements of the three-dimensional wind components, an open-path gas analyzer (Li7500, LI-COR) to obtain the air concentrations of H_2O and CO_2, an air temperature and humidity sensor (HMP45C, Vaisala), a four-component net radiometer (NR01, Hukseflux Thermal Sensors) for incoming and outgoing short- and long-wave radiation, a photosynthetically active radiation sensor (Li-190, LI-COR), and a heated standard Hellmann type tipping bucket rain gauge (Ecotech GmbH). The soil monitoring comprises multiple sensors for measuring soil

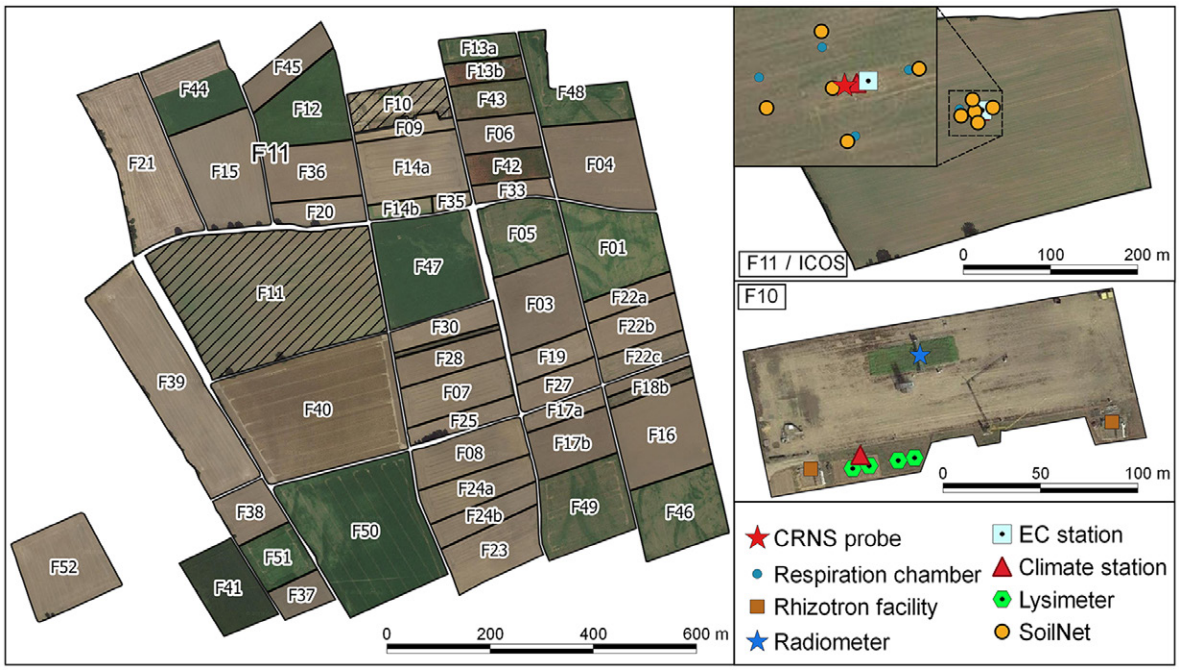

Fig. 3. Map showing fields and the instrumentation of the agricultural test site Selhausen. Data source: District Council Cologne (aerial photograph).

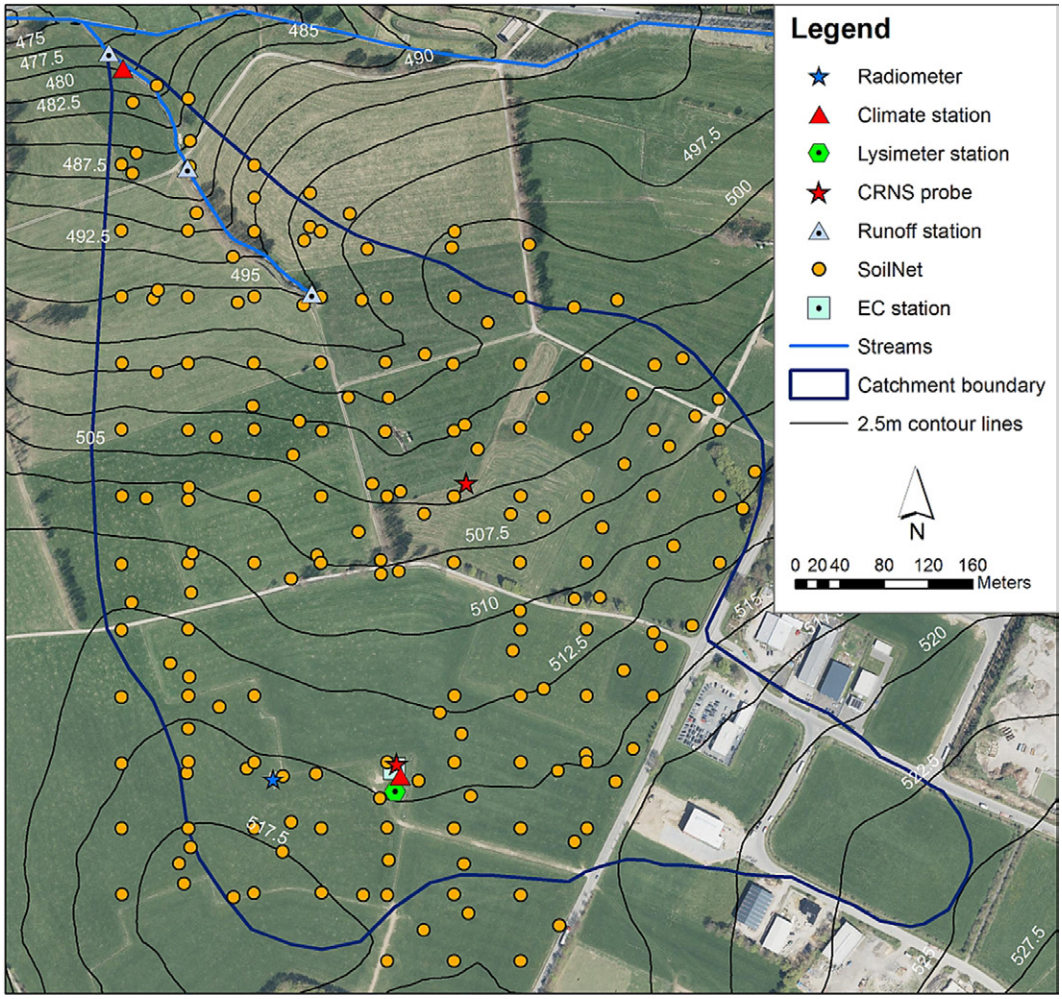

Fig. 4. Map showing the catchment and instrumentation of the Rollesbroich test site. Data source: District Council Cologne (aerial photograph).

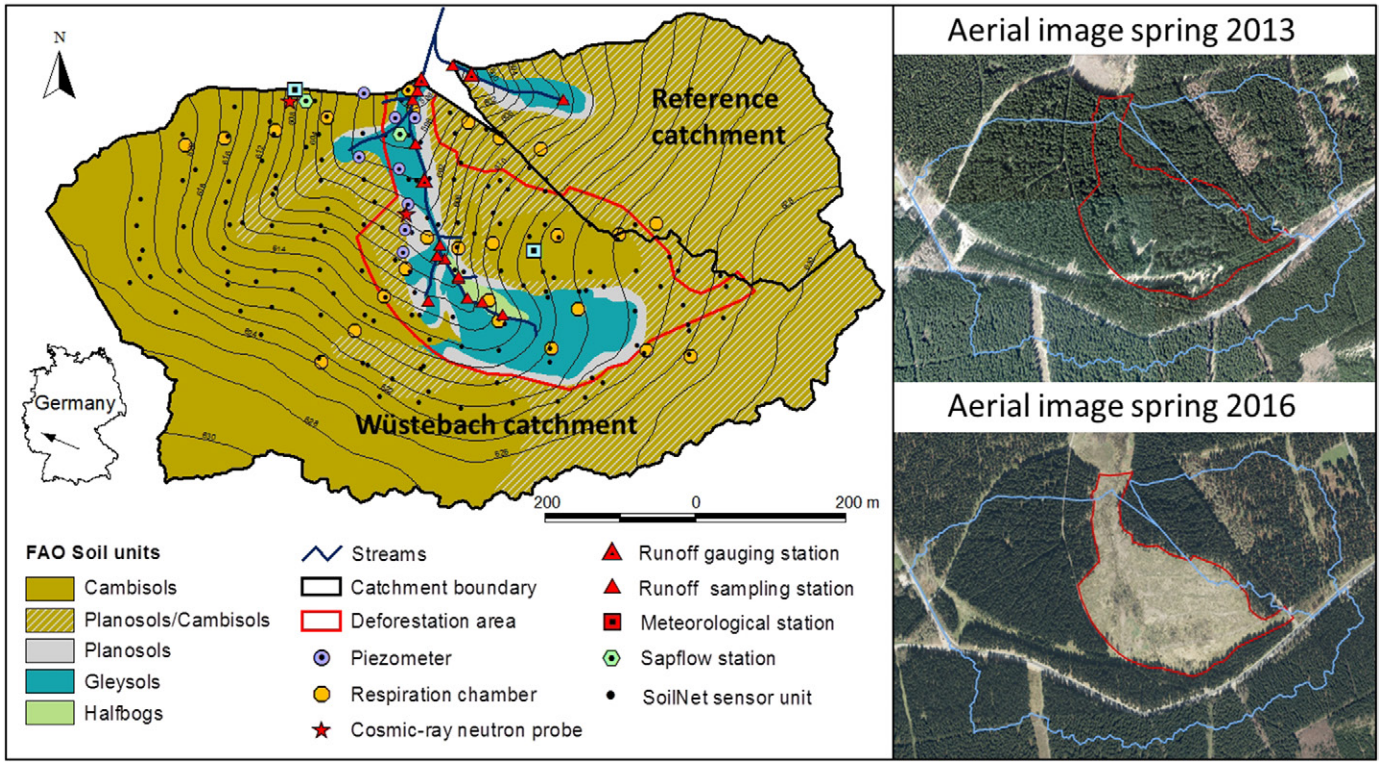

Fig. 5. Map showing major soil types and the instrumentation of the Wüstebach experimental catchment and the reference catchment as well as the deforestation area before and after the clear-cut. Data source: District Council Cologne (aerial photograph).

temperature (TCAV, Campbell Scientific), soil moisture (CS616, Campbell Scientific), and soil heat flux (HFP01, Hukseflux). The EC raw data are obtained with a sampling rate of 20 Hz using a high-performance datalogger (CR3000, Campbell Scientific). During post-processing, fluxes are aggregated to 30 min. The complete post-processing of the flux data, including established EC conversions and corrections, tests on high-frequency data as well as on processed 30-min fluxes, quality flagging, calculation of uncertainty estimates, and footprint assessments was in line with the standardized strategy for EC data calculation and quality assurance presented by Mauder et al. (2013). The EC station in Selhausen is maintained according to ICOS Level 1 standards (https://www.icos-ri.eu/). The continuous flux measurements by EC are amended by manual chamber measurements (Graf et al., 2013; Kupisch et al., 2015) and profile methods (Ney and Graf, 2018) at the Merzenhausen, Selhausen, and Wüstebach sites. These additional measurements are used both for cross-validation between methods and to investigate small-scale spatial heterogeneity of surface fluxes.

Weather Radars

Precipitation is additionally monitored in 5-min intervals by two dual polarized X-band Doppler weather radars (BoXPol and JuXPol). The BoXPol radar is installed on a 30-m-tall building in Bonn and operated by the Meteorological Institute of the University of Bonn. The JuXPol radar is part of TERENO and operated by the Agrosphere Institute of the Forschungszentrum Jülich GmbH. It is installed on top of the Sophienhöhe (Fig. 2), an artificial hill created from open-pit mining sediments that surmounts the surrounding terrain by roughly 200 m. Both weather radars use the DWSR-2001-X-SDP radar system (Enterprise Electronics Corporation) and Enigma signal processors (GAMIC GmbH). The radars provide precipitation data products with a radial resolution of 100 m (BoXPol) and 50 m (JuXPol). The data from both radars are merged to obtain a precipitation product with higher accuracy. For more technical details on both radars and the required data processing, see Diederich et al. (2015).

Network of Streamflow Observation Stations

Runoff is measured in the intensive experimental catchments Rollesbroich and Wüstebach using gauging stations equipped with a combination of a V-notch weir for low-flow measurements and a Parshall flume to measure normal to high flows (Qu et al., 2016; Bogena et al., 2015b). In addition, runoff data from 39 official runoff gauging stations (Fig. 2) operated by the local water associations (i.e., WVER, Wasserverband Perlenbach, Erftverband) are made available via the data exchange platform TEODOOR (see below).

To determine the water chemical status of the streams in the Wüstebach and Rollesbroich catchments and of the Erkensruhr River, the runoff gauging stations are intensively instrumented and regularly sampled (Fig. 2). Weekly grab samples are collected manually from several locations in the Wüstebach and Rollesbroich catchment. All samples collected for analysis of water chemistry

are filtered in the laboratory (0.45 μm) before major anions and cations are measured using ion chromatography (Cl^-, NO^{3-}, SO^{4-}, NH_4^+, and PO_4^{2-}) and inductively couple plasma–optical emission spectrometry (Al^{3+}, total Fe, Ca^{2+}, Mg^{2+}, Na^+, and K^+). Dissolved organic C (DOC) is measured as non-purgeable organic C together with dissolved total N (DTN) with a Shimadzu TOC-VCPN analyzer. The specific UV absorbance (SUVA) is calculated by normalizing the spectral absorption coefficient at 254 nm (SAC_{254}) by the DOC concentration. The SUVA is usually taken as a measure of the aromatic character of DOC and can also be a proxy for the DOC concentration itself.

Instrumentation of the runoff stations include multi-probe sensors (YSI 6820, YSI Inc.) to measure pH, electrical conductivity, temperature, and turbidity in streamflow and autosamplers (AWS 2002, Ecotech) that allow event-based sampling at higher temporal resolution. The outlet of the Wüstebach catchment and the runoff station at the Erkensruhr River are furthermore instrumented with an optical sensor (TriOS proPS) to monitor the SAC_{254}, stream-water turbidity, NO_3–N, and DOC concentrations.

Network of Cosmic-Ray Neutron Soil Moisture Stations

A network of 13 cosmic-ray neutron stations (CRNS; Zreda et al., 2012; Andreasen et al., 2017) is used to measure field-scale soil moisture (Fig. 2; Table 1). The CRNS network covers the relevant land use types and allows characterization of temporal soil moisture dynamics across the entire Rur catchment (Baatz et al., 2014). The CRNS are equipped with either a CRS-1000 or a CRS-2000/B cosmic-ray neutron probe (Hydroinnova LLC) that measure hourly neutron intensity. Conversion of neutron intensity into soil moisture has been described in detail by Bogena et al. (2013) and Baatz et al. (2015). The CRNS probes measure integral soil moisture in a circular footprint centered on the detector with a diameter ranging from 260 to 480 m (Köhli et al., 2015). The penetration depth decreases with increasing soil moisture and ranges from 55 to 15 cm for volumetric water content values ranging from 0.05 to 0.55 m^3/m^3 (Schrön et al., 2017). Ten CRNS started their operation between February 2011 and May 2012, and three additional CRNS were added in 2015. The CNRS transmit data wirelessly in near real-time to the TERENO database to support data assimilation and hydrological forecast modeling activities at the catchment scale.

Dedicated Experimental Sites

We now present the three intensive research sites Selhausen, Rollesbroich, and Wüstebach, which represent typical environmental conditions of the respective regions in the Rur catchment, i.e., intensive agriculture in the northern part and extensive agriculture and near-natural forest in the southern part.

The Selhausen Agricultural Station

The Selhausen agricultural research station (50.865°N, 6.447°E, about 100–110 m asl) consists of 51 agricultural fields covering an area of about 1 by 1 km (Fig. 3) and represents the heterogeneous rural area of the lower Rhine valley (main crops are sugarbeet, winter wheat, winter barley [*Hordeum vulgare* L.], maize, and rapeseed [*Brassica napus* L.]). This region belongs to the temperate maritime climate zone, with a mean annual temperature and precipitation of 10.2°C and 714 mm, respectively. The soil was classified as a Cambisol with a silty loam texture.

In spring 2011, one of the largest fields at the agricultural station was equipped with an EC station (see above). Besides flux measurements and typical meteorological parameters, the phenological development of the crops and farming activities are also recorded at a weekly to monthly basis. Groundwater level, water conductivity, and temperature in a groundwater well next to the

Table 1. Basic information on the cosmic ray neutron sensor network (location, date of installation, and calibration information); see also Baatz et al. (2014).

Station name	Location	Start of measurement	N_0 parameter†	Bulk density	Lattice water	Thermal counter
				g/cm^3	m^3/m^3	
Aachen	50.7985 N, 6.0247 E	13 Jan. 2012	1174	1.20	0.06	
Gevenich	50.9892 N, 6.3235 E	7 July 2011	1206	1.31	0.03	yes
Heinsberg	51.0411 N, 6.1042 E	9 Sept. 2011	1242	1.27	0.04	yes
Kall	50.5013 N, 6.5264 E	15 Sept. 2011	1268	1.31	0.09	
Kleinhau-Hürtgenwald	50.7224 N, 6.3720 E	26 Aug. 2015	899	1.12	0.06	yes
Merzenhausen	50.9303 N, 6.2974 E	19 May 2011	1202	1.39	0.04	yes
Rollesbroich	50.6219 N, 6.3042 E	19 May 2011	1208	1.09	0.07	yes
RollesbroichN	50.6241 N, 6.3051 E	22 May 2012	1081	1.09	0.07	yes
RurAue	50.8623 N, 6.4273 E	8 Nov. 2011	1109	1.12	0.05	
Schöneseiffen	50.5149 N, 6.3755 E	15 Aug. 2015	941	1.11	0.05	yes
Selhausen	50.8659 N, 6.4471 E	4 Mar. 2015	1007	1.26	0.04	yes
Wildenrath	51.1327 N, 6.1691 E	7 May 2012	988	1.15	0.03	
Wüstebach	50.5034 N, 6.3330 E	20 Mar. 2011	936	0.83	0.07	yes

† Calibration parameter of the standard cosmic ray neutron probe calibration function.

EC station are continuously measured using a multi-probe (CTD, Decagon Devices). Since 2015, four automated closed dynamic chambers (Li-8100, LI-COR) have been continuously operated to measure CO_2 emissions from the soil. In addition, a SoilNet wireless sensor network consisting of five profiles (depths of −0.01, −0.05, −0.1, −0.2, −0.5, and −1 m) is operated in this field to measure soil moisture and soil temperature (SMT100, Trübner Precision Instruments) and soil heat flux (HFP01, Hukseflux Thermal Sensors) in near real-time. From 2015 to 2018, the site hosted field campaigns for the comparison of methods to determine flux components, e.g., the contribution of evaporation and transpiration to evapotranspiration, including isotope, microlysimeter, and profile (Ney and Graf, 2018) measurements.

In 2010, a set of 18 lysimeters (UMS GmbH) was installed to continuously determine water balance components with high precision (see below). In addition, two rhizotron facilities were built (Fig. 3) that enable root growth observations and soil moisture monitoring with ground-penetrating radar (GPR) in both lateral (7-m-long boreholes) and vertical (six depths) directions during a crop growing cycle (Cai et al., 2016).

The Rollesbroich Experimental Catchment

The Rollesbroich grassland experimental catchment is located in the Eifel mountain range and covers an area of about 40 ha, with altitudes ranging from 474 to 518 m asl and an average slope of 1.63° (Fig. 4). The mean annual air temperature and precipitation are 7.7°C and 1033 mm, respectively. The dominant soils are Cambisols in the southern part and Stagnosols in the northern part of the catchment. The grassland vegetation is dominated by perennial ryegrass (*Lolium perenne* L.) and smooth meadow grass (*Poa pratensis* L.).

The Rollesbroich catchment is a reference site for the validation of remote sensing data products (e.g., Hasan et al., 2014; Montzka et al., 2013a, 2016) and hydrological models (e.g., Gebler et al., 2017). To this end, all components of the water balance (e.g., precipitation, evapotranspiration, runoff, soil water content, and drainage) are continuously monitored using state-of-the-art instrumentation, providing detailed information about the spatial and temporal variation of all water balance components. This integrated data set has been used to investigate interactions between the land surface and the atmosphere (e.g., Gebler et al., 2015; Post et al., 2015; Zhang et al., 2017). Recently, a 20-m-high tower with a passive ELBARA II L-band radiometer (Gamma Remote Sensing AG) was installed (Fig. 4). A detailed description of the instrumentation within the Rollesbroich experimental catchment and the available hydrological data has been provided by Qu et al. (2016) and Groh et al. (unpublished data, 2018).

The Wüstebach Deforestation Experiment

This experiment investigates the effects of clear-felling of a spruce forest on hydrological processes in the Wüstebach catchment (Fig. 5; Bogena et al., 2015b). The Wüstebach catchment covers an area of ∼38.5 ha, with altitudes ranging between 595 and 628 m asl and an average slope of 3.6%. The geology is dominated by Devonian shales covered by a periglacial solifluction layer of about 1- to 2-m thickness in which Cambisols and Planosols have developed on the hillslopes and Gleysols and Histosols have formed under the influence of groundwater in the valley. The main soil texture is silty clay loam. The mean annual precipitation is 1220 mm (Bogena et al., 2010), and the main vegetation is Norway spruce [*Picea abies* (L.) H. Karst.] planted in 1946. During the late summer of 2013, trees were almost completely removed in an area of 9 ha near the main Wüstebach stream to initiate the regeneration of near-natural beech (*Fagus sylvatica* L.) forest.

The hydrological observation system in the Wüstebach catchment includes three runoff stations and eight groundwater piezometers. At several locations along the Wüstebach stream, water temperature, pH, redox potential, and electrical conductivity are manually measured using field instruments (WTW, Xylem Inc.), and water samples are collected for analysis of water chemistry on a weekly basis (see also above). The runoff stations are equipped with multi-probes (YSI 6820, YSI Inc.) that measure water temperature, pH, and electrical conductivity every 15 min, and autosamplers (AWS 2002, Ecotech) with an hourly sampling interval are installed at all runoff gauging stations.

In 2010, a 37-m-high meteorological tower was installed in the northwest corner of the catchment. The tower is equipped with profiles (8, 16, 24, 27, and 32 m) of two-dimensional sonic anemometers (WindSonic, Gill Instruments) and ventilated thermometers for measuring wind speed, wind direction, and air temperature, respectively. A four-component net radiometer (NR01, Hukseflux Thermal Sensors) for incoming and outgoing short- and long-wave radiation, and a photosynthetically active radiation sensor (SKP215, Llandrindod Wells) is installed on a 5-m-long boom at 34 m above ground. At the ground, these tower measurements are complemented by measurements of snow depth (SR50A, Campbell Scientific), stem and surface temperature (IR120, Campbell Scientific), soil heat flux (HFP01, Hukseflux Thermal Sensors), and a soil profile (depths of −0.02, −0.05, −0.1, −0.2, −0.5 and −1 m) of soil moisture (CS616, Campbell Scientific) and soil temperature (TCAV, Campbell Scientific) measurements.

In September 2013, a second EC station was set up in the center of the clear-felling area. Additionally, regular manual chamber measurements of soil CO_2 efflux with a closed dynamic chamber system (LI-8100-101, LI-COR Biosciences) and small-scale net CO_2 exchange and evapotranspiration with a flow-through chamber (Graf et al., 2013) were performed (Ney et al., unpublished data, 2018). Sapflow fluxes as a proxy for tree transpiration are measured every 30 min at six trees using Granier-type sensors (Rabbel et al., 2018).

A wireless SoilNet soil moisture sensor network with 600 ECH$_2$O EC-5 and 300 ECH$_2$O 5TE sensors (Decagon Devices; Rosenbaum et al., 2010) measures soil moisture and temperature every 15 min at 150 locations at the 5-, 20-, and 50-cm depths (Fig. 5; Bogena et al., 2010). Soil physical and chemical properties

were determined by a soil sampling campaign 1 mo prior to deforestation, with a total of 143 sampling locations according to the existing SoilNet network (Bogena et al., 2015b). From each sampling location, five undisturbed HUMAX liners (Martin Burch AG) and three bags with disturbed soil samples of the L/Of, Oh, and Ah horizons were taken. All samples were analyzed for pH, nutrient content, and relevant elemental content compositions and their stable isotope values (Gottselig et al., 2017; Wu et al., 2017). Further soil sampling was performed after the deforestation in 2014 and 2015 for the analysis of clear-cut effects on biological P cycling (Siebers et al., 2018). The Wüstebach catchment has been used as a reference site for the application of various hydrological models, e.g., HydroGeoSphere (Cornelissen et al., 2016, 2014), MIKE-SHE (Koch et al., 2016), and ParFlow-CLM (Fang et al., 2015, 2016; Rahman et al., 2016).

Dedicated Observations

We now present examples of more dedicated observations (e.g., using various geophysical techniques, stable isotope analysis, on-site weighable lysimeter stations, and airborne microwave remote sensing) that focus on more specific research questions and/or environmental settings of the Rur catchment.

Geophysical Observations

Ground-penetrating radar and electromagnetic induction (EMI) measurements can be used to noninvasively investigate the structure, composition, and hydraulic state of the subsurface. At the Selhausen test site (Fig. 3), large-scale investigations of agricultural fields in an area of 1 by 1 km were performed by using multi-coil EMI systems pulled by an all-terrain vehicle equipped with GPS positioning. These multi-coil EMI systems provide apparent electrical conductivity (ECa) values for several depths of investigation (DOIs). The Selhausen area is characterized by a series of river terraces, where satellite-based leaf area index data (RapidEye) obtained after a dry period showed distinct patterns due to the presence of paleochannel structures in the subsurface of the upper terrace (see Fig. 6). It could be shown that these patterns in leaf area index correlated well with ECa patterns obtained for the deepest DOI (Rudolph et al., 2015), indicating that the deeper subsoil is responsible for the good crop performance in times of water scarcity for this particular area. When comparing crop development and ECa patterns during the growing season, correlations were strongest when the soil was dry (Stadler et al., 2015). To further improve the interpretation of EMI data, we inverted the EMI data to obtain a quasi-three-dimensional model of the subsurface EC distribution (von Hebel et al., 2014) after appropriate calibration of the EMI measurements. In a next step, multi-configuration EMI measurements were made at 51 agricultural fields in the Selhausen area (Fig. 3). After combining this EMI survey with optimized sparse soil sampling and a remote-sensing-based classification methodology, a high-resolution (meter-scale) soil map with 18 soil types was obtained (Brogi et al., unpublished data, 2018). Electromagnetic induction measurements were also performed at the forested Wüstebach catchment, where time-lapse ECa maps were spatially consistent but temporally inconsistent with catchment-wide soil moisture data provided by a wireless soil moisture sensor network (Altdorff et al., 2017).

Stable Isotope Observations

The stable oxygen and hydrogen isotope ratios ($\delta^{18}O$ and $\delta^{2}H$) are used as hydrological tracers to investigate hydrological flow paths and water transit times in the Rur catchment (e.g., Stockinger et al., 2014, 2015, 2016, 2017). To elucidate catchment-wide water

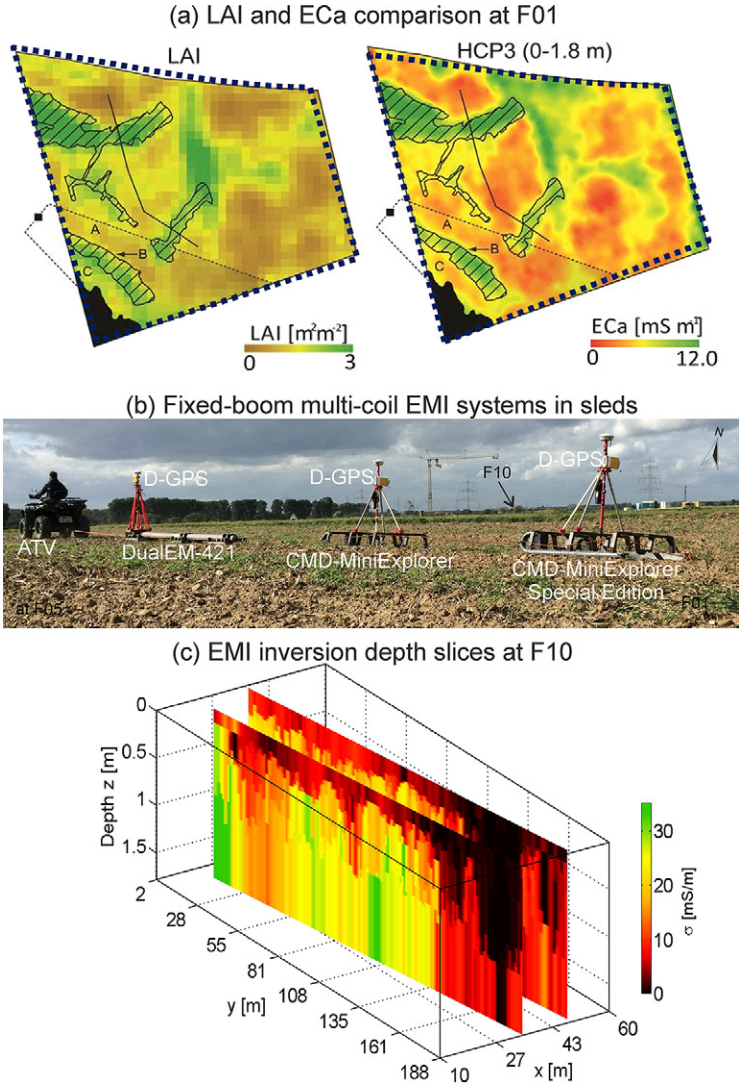

Fig. 6. (a) Comparison of leaf area index (LAI) and apparent electrical conductivity (ECa) at Field F01 (Rudolph et al., 2015), (b) electromagnetic induction (EMI) measurement setup showing three EMI sleds at Field F05, and (c) depth slices through quasi-three-dimensional EMI inversion result at Field F10 (von Hebel et al., 2014), showing the low electrically conductive eastern part due to a massive gravel layer as well as the plow horizon over the test site and generally increasing electrical conductivity with increasing depth in the western part due to loamy soil.

transport for small- and mesoscale catchments, samples of different components of the hydrological water cycle (precipitation, throughfall, soil solution, and stream water) are taken and analyzed in several subcatchments of the Rur catchment (Fig. 2). Weekly precipitation samples for isotopic analysis are collected by wet deposition collectors at the meteorological station Schöneseiffen and the Erkensruhr runoff gauging station. In addition, precipitation below the forest is sampled using throughfall samplers (RS200, UMS GmbH) situated in the Wüstebach catchment and in a deciduous forest approximately 10 km north of the Wüstebach catchment. Stream water isotope information is determined from samples taken by autosamplers (AWS 2002, Ecotech), and weekly water grab samples are taken at the Wüstebach, Rollesbroich, and Erkensruhr runoff gauging stations. To investigate the mixing of stable water isotopes in the unsaturated zone, two suction cup arrays are used to sample soil water in the hillslope and the riparian zones at three different depths in the Wüstebach catchment. Finally, isotope concentrations are also regularly determined in the sample leachates of the lysimeter stations (see below). All water isotopic analyses are performed using laser-based cavity ring-down spectrometers (L2120-i and L2130-i, Picarro).

Network of Lysimeter Stations

A network of six lysimeter stations has been installed in the Rur catchment (three at Selhausen, two at Rollesbroich, and one at Wüstebach) to determine precipitation, actual evapotranspiration (resolution of 0.01 mm), change in soil water storage, leachate, and upward directed water flow from capillary rise (Pütz et al., 2016). Each lysimeter station features six lysimeters that are arranged in a hexagonal design around the centrally placed service unit hosting analytical and data recording devices. The lysimeters are made of stainless steel, with a surface area of 1.0 m^2 and a length of 1.5 m. All lysimeters were filled with monolithic soil cores. Vegetation on the lysimeters is natural grassland with and without management or cereal crop rotation. The lower boundary condition of each lysimeter is controlled using parallel suction racks that were installed after the lysimeter was filled. These suction racks ensure that water will drain from the lysimeter when the matric potential at the bottom of the lysimeter is higher than in the surrounding control area. Leachate is collected in a weighable tank. If the matric potential at the bottom of the lysimeter is lower than in the surrounding control area, water is pumped back into the lysimeter from this tank. Thus, lysimeter observations can mimic capillary rise from deeper soil layers or shallow groundwater tables, which can serve as an additional water supply for evapotranspiration processes (Schwaerzel and Bohl, 2003; Groh et al., 2016). Water balance components are determined from the change in weight of each lysimeter using a precision scale. Lysimeter weight changes are affected by external disturbance factors like wind, management, and animals. Thus, the derivation of highly resolved water balance components requires an appropriate data processing scheme, including visual and automatic plausibility checks and a noise reduction filter (Peters et al., 2017). In addition, matric potential sensors, tensiometers, temperature sensors, heat flux plates, soil moisture content, and CO_2 sensors were installed at different soil depths (10, 30, 50, and 140 cm). Finally, soil solution is extracted at depths of 10, 30, and 50 cm with a constant vacuum of 100 hPa. All measured data are logged on-site and sent to a central server using a GPRS modem.

Remote Sensing Activities

Various ground-based measurement techniques and their monitoring networks have been utilized for the validation of remote sensing products, which are becoming more strategic for global monitoring of Earth resources (Mohanty et al., 2017). Multispectral remote sensing data have been used in water balance and N transport simulations in the Rur catchment (Montzka et al., 2008a, 2008b). Ali et al. (2015) developed methods to retrieve plant properties (i.e., leaf area index) for the Rur hydrological observatory from multispectral satellite data (RapidEye) at high spatiotemporal resolution, which was used for the analysis of vegetation heterogeneities (Reichenau et al., 2016; Rudolph et al., 2015) and for the simulation of net ecosystem exchange (Post et al., 2018).

In the framework of the European Space Agency Soil Moisture and Ocean Salinity (SMOS) mission launch in 2009 (Kerr et al., 2010), airborne campaigns were conducted with the EMIRAD and PLMR (Polarimetric L-band Multi-beam Radiometer) radiometers. The campaigns took place also prior to the satellite launch in 2009 to analyze different soil moisture retrieval methods. Montzka et al. (2013a) used data from airborne remote sensing campaigns with EMIRAD and the HUT-2D radiometers in the Rur catchment to validate SMOS soil moisture products. Data from airborne campaigns with the PLMR2 radiometer were used to analyze a Monte Carlo approach for simultaneous retrieval of vegetation opacity and soil moisture (Hasan et al., 2014).

The Rur hydrological observatory contributes to the Soil Moisture Active and Passive (SMAP) mission validation activities by operationally providing soil moisture reference data (Colliander et al., 2017). In addition, simultaneous passive and active microwave airborne campaigns were conducted in the Rur catchment by the German Aerospace Center (DLR) using a dedicated platform (see Fig. 7). These unique data were used to analyze various radiometer–radar fusion methods for retrieving improved soil moisture data products for the Rur hydrological observatory (Montzka et al., 2016). In addition, alternative methods for downscaling SMAP radiometer data have been recently tested (Montzka et al., 2018).

Further remote sensing activities in the Rur hydrological observatory include validation of ASCAT and SMOS with hydrological simulations (Rötzer et al., 2014), validation of various satellite soil moisture data products (ASCAT, AMSR2, SMAP, and SMOS) using data from the cosmic-ray neutron network established in the Rur hydrological observatory (Montzka et al., 2017), and using remote sensing data for hydrological modeling of the Rur catchment (Han et al., 2013, 2014; Montzka et al., 2013b).

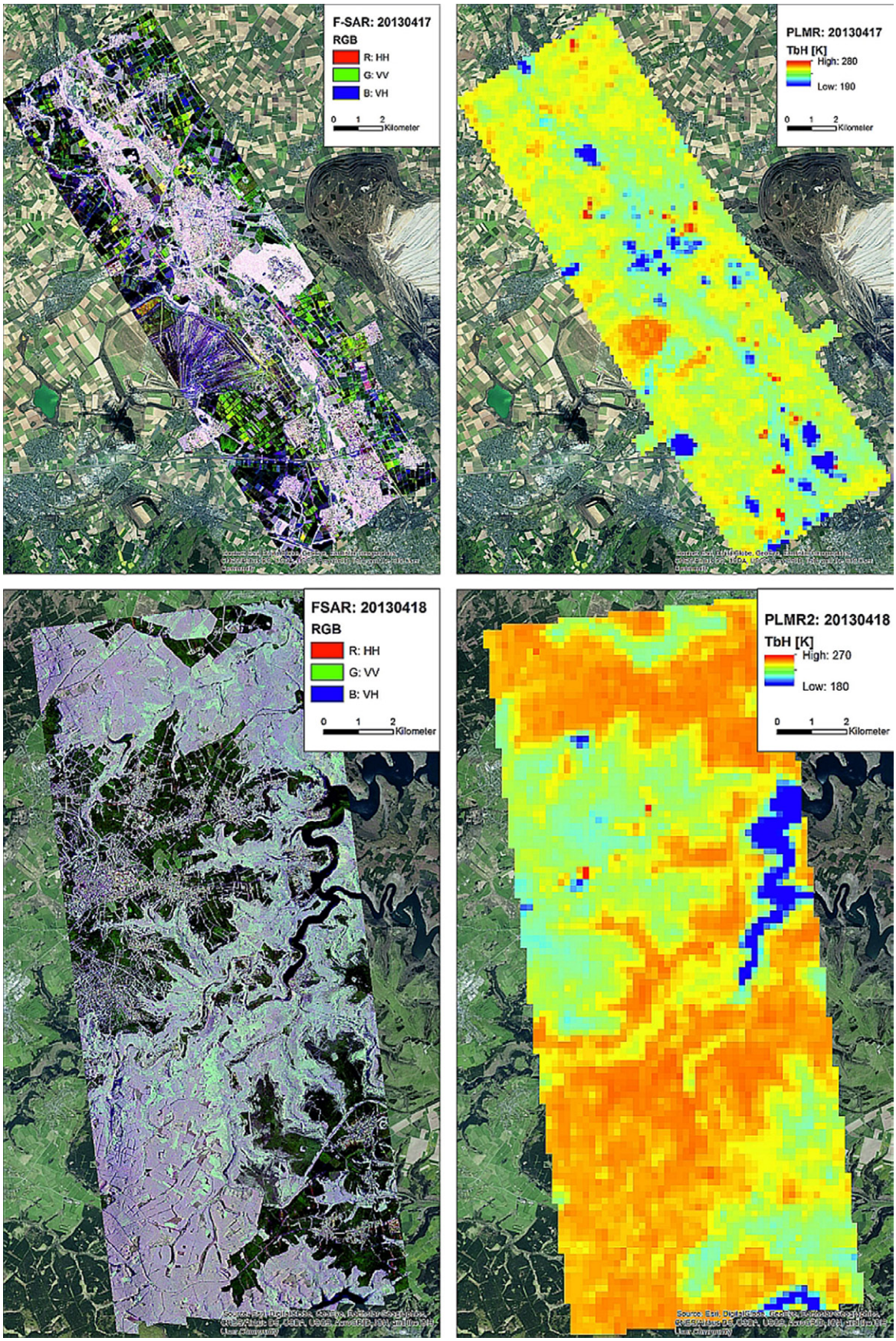

Fig. 7. Radar observations (left) and radiometer observations (right) for Jülich (top) and the Eifel region (bottom) recorded on 17 and 18 Apr. 2013, respectively. Data source: District Council Cologne (aerial photograph).

Data Management and Policy

The Rur hydrological observatory constantly produces a large number of complex data sets that need to be managed and archived in a timely manner. The data collected from automatic climate and runoff stations, eddy covariance stations, SoilNet networks, and SoilCan lysimeters is estimated to be around 150,000 measurements per hour. In addition, the weather radar produces large amounts of raw data and processed data (~500 MB per hour). To be able to process these continuous data streams, methods for regular plausibility checks and effective tools for automated data storage and archiving have been developed in the framework of the TERENO project (Devaraju et al., 2014, 2015). In addition to the data quality, the adequate description of the data stocks via metadata plays a decisive role. For this reason, data are always treated as a combination of data and descriptive metadata. A common TERENO metadata profile ensures uniform data description within the TERENO network.

In addition to its role as a common information and exchange platform for the TERENO network, the TEODOOR portal (http://www.tereno.net) has the function of bringing together and publishing the data from the hydrological observatory. This is done by a number of tools, including a hierarchical keyword search and WebGIS functionalities that allow the user to obtain detailed insights into the data availability of all experimental sites and networks. Data visualization tools make it possible to select, display, and check all data types from different time periods. Finally, TEODOOR enables access to the data in compliance with the common TERENO data policy.

New Insights and Novel Scientific Findings

In the following, we present example key findings of the ongoing interdisciplinary research work in the Rur hydrological observatory, covering a wide range of topics: analysis of hydrological processes using stable isotopes and DOC, analysis of deforestation effects on terrestrial processes, analysis of subsurface structures and soil moisture variability, and data assimilation for catchment modeling.

Using Stable Isotopes to Analyze Runoff Processes in the Wüstebach Catchment

Using the stable isotopes of water as a tracer in combination with a conceptual rainfall–runoff model revealed that the transit time of precipitation in the Wüstebach catchment is influenced by the ratio of the riparian to the hillslope zones (Stockinger et al., 2014). An increase in the riparian area of the Wüstebach catchment led to faster transit times. Additionally, it was found that hillslopes disconnect from runoff-generating processes under dry catchment conditions because new water from precipitation is consumed by the spruce forest. Using the isotopic data of open precipitation and throughfall, it was further shown that canopy interception induced changes in the isotope values of throughfall that influenced not only modeled transit time distributions (Stockinger et al., 2015) but also the tracer-derived fraction of young water (Stockinger et al., 2017) (Fig. 8).

Moving to a larger catchment scale, two time series of different temporal resolutions of tracer data (weekly and subdaily) were used for the Erkensruhr catchment (Fig. 2) to show that a coarser temporal resolution leads to a loss of information about short transit times (Stockinger et al., 2016). This study emphasized the need for high-resolution observations in hydrology, as many studies use weekly isotope tracer data. Current work focuses on high-resolution automatic measurements of stable water isotopes at the outlet of the Erkensruhr River with the aim to better understand the changes in transit time distributions during single stormflow events.

Linking Dissolved Organic Carbon and Nitrate Export in the Wüstebach Catchment

Our hydrochemical long-term observations in the Wüstebach catchment and its tributaries revealed a remarkable linkage between seasonally varying concentrations of DOC and NO_3^- and their ratios at the respective sampling points and the $\delta^{18}O$ values of the discharge (Weigand et al., 2017; Stockinger et al., 2015). Water transit times derived from $\delta^{18}Oc$ values were strikingly correlated with DOC and NO_3^- concentrations in such a way that lower C/N ratios coincided with longer water transit times, indicating a substantial groundwater contribution to the surface water at the respective sampling points.

The importance of the contribution of storm events to the annual export of DOC and DTN via surface water from the Wüstebach catchment became evident from an analysis of subdaily hydrochemical data. Stream water samples were collected in 4-h intervals using an autosampler located at the main gauging station (Fig. 5) during a 2-wk period of combined snowmelt and

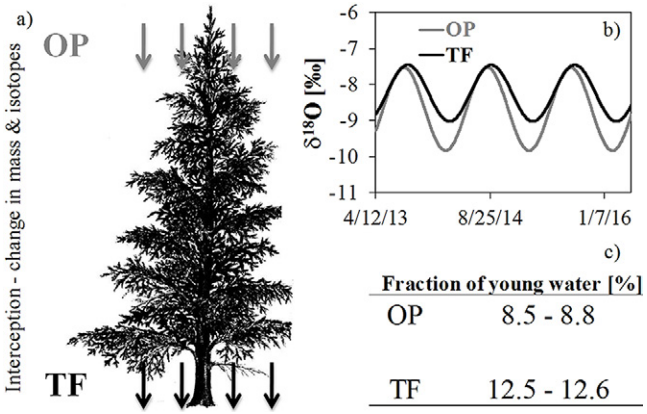

Fig. 8. (a) Canopy interception causes a change in mass and isotopic composition of open precipitation (OP) while generating throughfall (TF); (b) these changes influence the shape of the sine wave fitted to the respective precipitation data and that is used to calculate the fraction of young water (Fyw); (c) accordingly, the respective Fyw values derived from these different sine waves deviate considerably (adapted from Stockinger et al., 2016).

heavy rainfall in January 2011. The hydrochemical data revealed that during this event about 42 and 37% of the total annual load of DOC and DTN, respectively, were exported (Table 2). These enormous amounts are not only due to the increase in hydraulic discharge during a storm event but also rooted in the transient increase in concentrations of DOC and DTN occurring especially during the initial hours of such an event. This bias of underestimating exports if calculations are based on weekly grab samples must be faced by continuous monitoring of DOC and DTN. Because this is not feasible with conventional methods, photometrically monitored SAC_{254} and NO_3^- concentrations can serve as measures for DOC and DTN, respectively.

Table 2. Total discharge, as well as dissolved organic C (DOC) and dissolved total N (DTN) loads, at Wüstebach catchment outlet in 2011 and during a single storm event in January 2011.

Parameter	Year 2011	Storm event (Jan. 2011)
Discharge, m^3	254	87 (34%)
DOC, kg	505	214 (42%)
DTN, kg	591	218 (37%)

Effect of Deforestation on Water Balance of the Wüstebach Catchment

The hydrological observations described above jointly enabled an analysis of the water budget of the Wüstebach catchment during the 3 yr prior to the partial deforestation, as a baseline for assessing immediate and long-term changes occurring after the deforestation. Precipitation, evapotranspiration, and discharge closed the catchment water budget to within 2% on a 3-yr basis and to within 9% for each of the individual years (Graf et al., 2014). On a weekly basis, changes in soil water storage measured by the SoilNet sensor network (see above) were correlated to the corresponding short-term residuals of precipitation, evapotranspiration, and discharge. Two typical soil moisture patterns could be identified, corresponding to more uniformly wet conditions throughout the catchment and drier situations, where high moisture in the topsoil was maintained only in the riparian zone shown by Stockinger et al. (2014) to remain connected to runoff generation throughout the year (see also below). After the deforestation of 22% of the catchment, the water budget of the catchment remained closed (residuals $\leq$8% on an annual basis) when evapotranspiration was calculated as the area-weighted average between the forest EC station and the newly installed EC station in the center of the clear-cut (Fig. 9; Wiekenkamp et al., 2016a). Actual evapotranspiration in the deforested area was reduced to about half the actual evapotranspiration of the forest during the first year after deforestation. This led to higher soil moisture in the clear-cut area and an increased annual runoff coefficient of the total catchment (69% in 2014 compared with an average value of 58% between 2011 and 2013). This runoff coefficient agrees well with observations of the Wüstebach lysimeter station installed in a forest meadow in 2014 (72%; Groh et al., 2018). Already in the second year after deforestation, the water budget components showed a strong tendency to return toward pre-deforestation values (Fig. 10). In contrast, CO_2 fluxes continued to show strong differences between the two areas in the fourth year after deforestation (Ney et al., unpublished data, 2018).

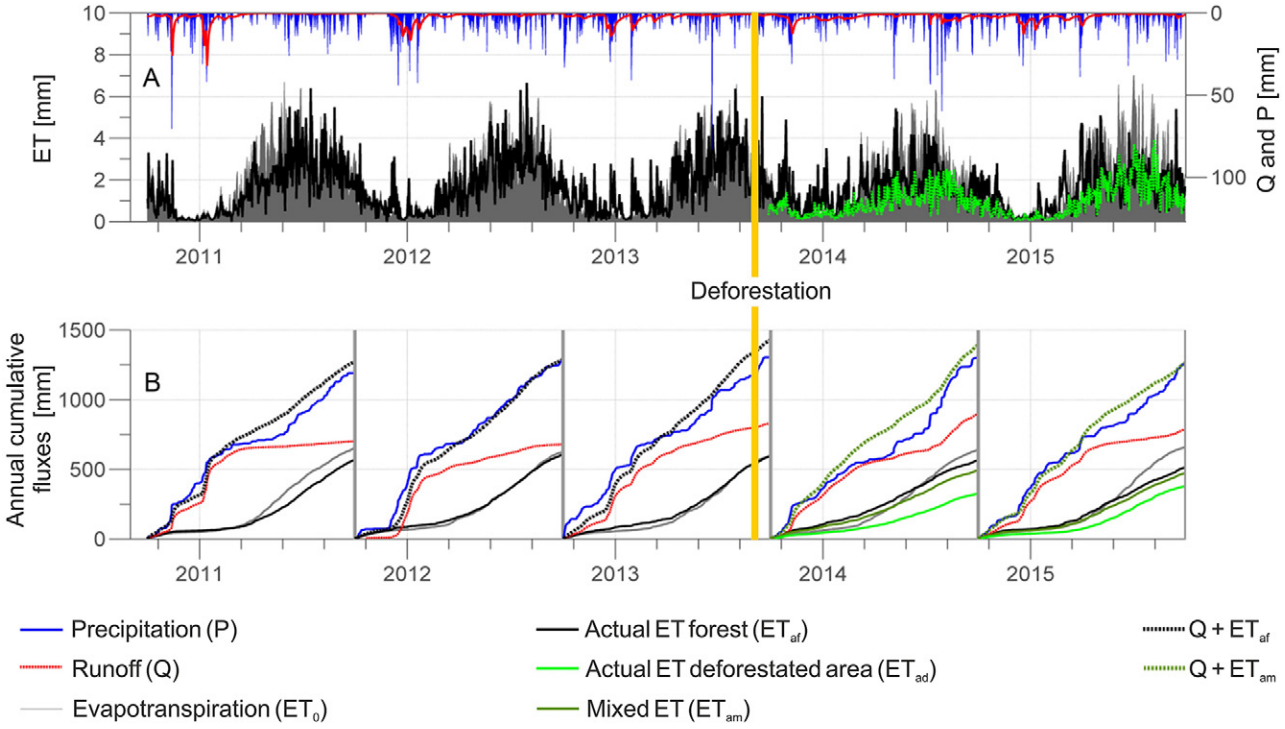

Fig. 9. Yearly cumulative water balance 3 yr before and 2 yr after deforestation in the Wüstebach catchment. The evapotranspiration of the forested area (ETaf), the deforested area (ETad), and the area-averaged evapotranspiration (ETam) are plotted separately (adapted from Wiekenkamp et al., 2016a).

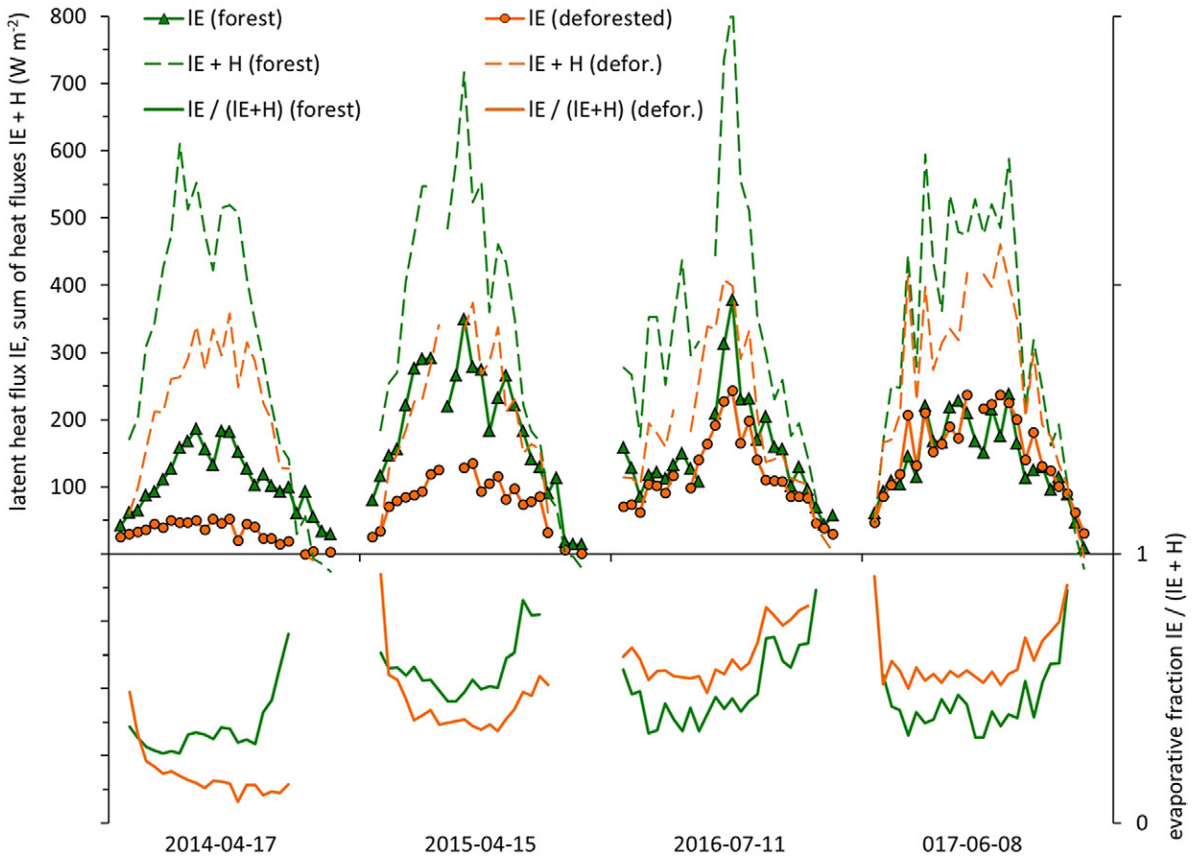

Fig. 10. Evapotranspiration as latent heat flux (lE) and sensible heat flux (*H*) during four selected days (6–20 UTC) with similar available energy, one from each year after the deforestation. Reduced evapotranspiration from the clear-cut during the first 2 yr was caused not only by reduced transpiration efficiency but also by lower available energy, as can be seen from the evaporative fractions lE/(lE + *H*). The difference in available energy results from a higher albedo and soil heat flux at the deforested site (not shown). While shown days represent typical forest clear-cut comparisons for each year, a reverted relation was found occasionally even during the first 2 yr, e.g., shortly after rainfall when near-surface soil moisture at the clear-cut enhanced evaporation.

Investigations of Soil Moisture Variability Using Sensor Network Data

The wireless sensor networks installed in the Rur hydrological observatory have been used extensively to understand the spatiotemporal variability of soil moisture at the catchment scale. For instance, Rosenbaum et al. (2012) studied the spatiotemporal dynamics of soil moisture in the Wüstebach catchment using data from the SoilNet sensor network described above. They found hysteretic effects in the relationship between spatial variability and mean catchment wetness at the event and seasonal time scales and as a function of the wetting–drying status of the catchment and precipitation conditions. Qu et al. (2014) analyzed the temporal stability of soil moisture observed by the wireless sensor network installed in the Rollesbroich catchment. They found that both soil moisture and saturation degree showed temporally stable characteristics that were correlated with the spatial variation in hydraulic parameters. In a subsequent study, Qu et al. (2015) developed a new closed-form expression to predict the local variability of soil water content and to estimate the spatial variability of hydraulic properties based on sensor network data from Wüstebach and Rollesbroich, as well as other data sources. Wiekenkamp et al. (2016b) used soil moisture sensor response times from the SoilNet sensor network to investigate controls on preferential flow in the Wüstebach catchment. They found that the spatial occurrence of preferential flow was mainly governed by small-scale soil and biological features and local processes, and showed no obvious relationship with spatial parameters (i.e., hydrological, topographical, and soil physicochemical parameters). Finally, Wiekenkamp et al. (2016a) used data from the same sensor network to analyze the spatiotemporal distribution of soil moisture before and after the partial deforestation of the Wüstebach catchment. They found that soil moisture in the deforested area was significantly higher than in the forested part, especially during the summer period (Fig. 11), which in turn caused an increase in the frequency of high discharge. These examples illustrate how detailed spatiotemporal soil moisture monitoring using wireless sensor networks can provide new insights into hydrological processes at the catchment scale.

High-Resolution Aquifer Characterization Using Full-Waveform Inversion of Cross-Hole GPR Data

Vertical borehole GPR measurements at the Krauthausen test site close to Selhausen were performed to investigate hydrogeological subsurface structures (Gueting et al., 2015). By combining several cross-hole planes, a section of 50-m length, 25-m width,

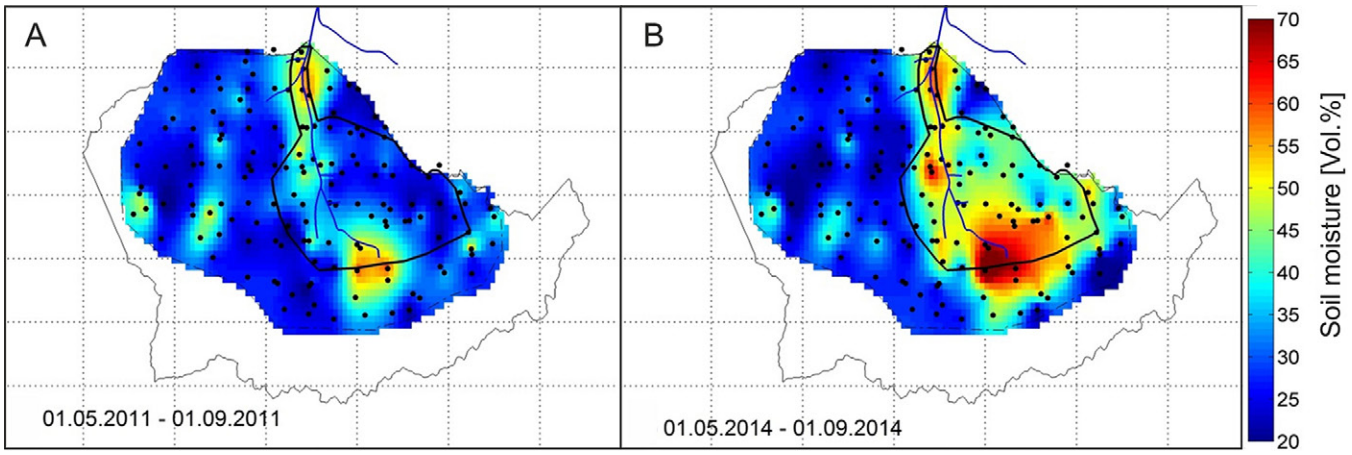

Fig. 11. Mean soil moisture for (A) 2 yr prior to the deforestation and (B) 2 yr after deforestation. As a reference, the deforested area within the catchment is marked on both maps (adapted from Wiekenkamp et al., 2016a).

and 10-m depth was investigated using conventional ray-based and full-waveform inversion of GPR measurements. The full-waveform inversion of all cross-sections (see Fig. 12) resulted in a high-resolution image of subsurface heterogeneity, where the observed decimeter-scale variability was able to explain the previously observed splitting of a tracer plume (Müller et al., 2010; Gueting et al., 2017). Since the GPR full-waveform inversion identified a hydraulically low-conductivity thin sand layer with a thickness of only a few decimeters that was not resolved by conventional ray-based GPR inversion, we conclude that the improvement in spatial resolution when using full-waveform GPR inversion is crucial to detect small-scale aquifer structures that are highly relevant for solute transport.

Hydrological Modeling and Data Assimilation

An important question is whether observations at a limited number of points allow a catchment-wide improvement of the characterization of hydrological states and fluxes. This research

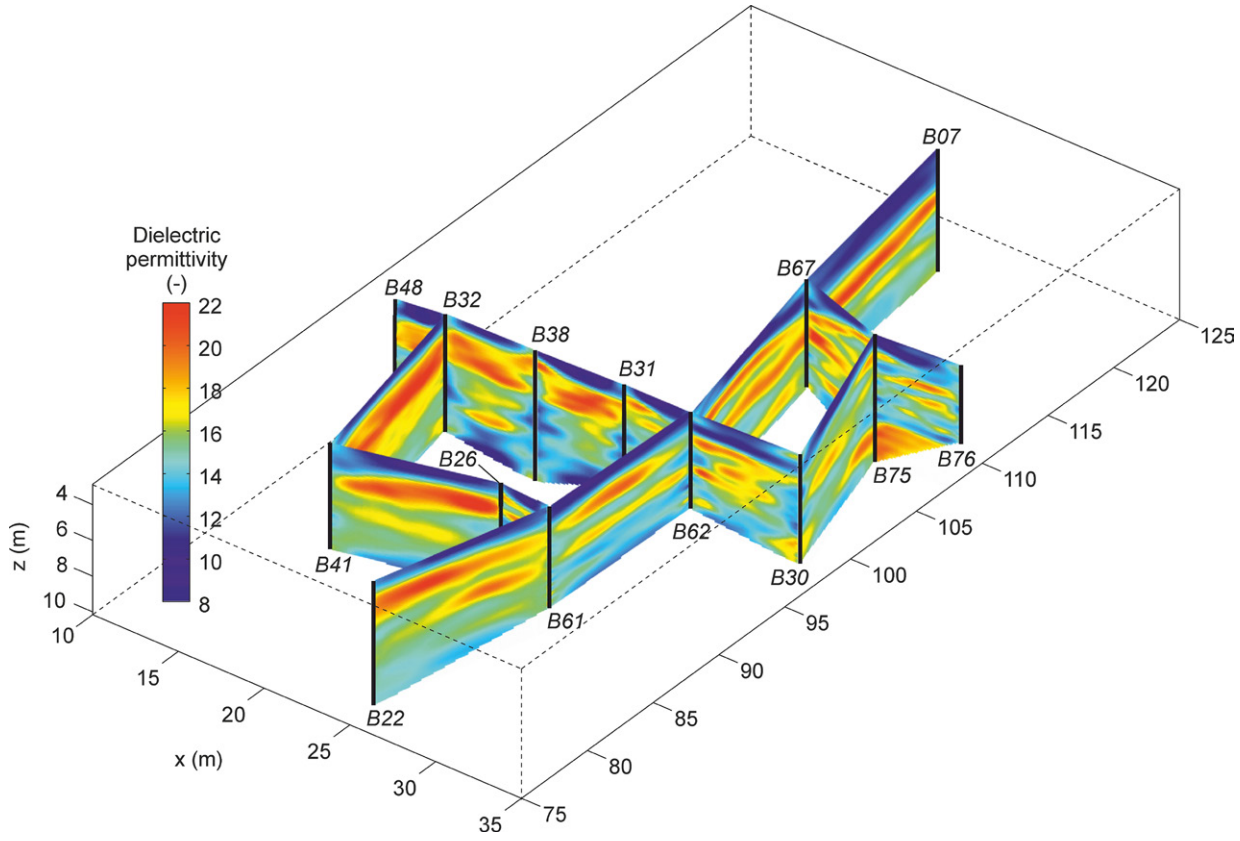

Fig. 12. Aquifer characterization using large-scale full-waveform cross-hole GPR data inversion showing detailed aquifer structures relevant for solute transport (modified after Gueting et al., 2017).

question was recently addressed by Baatz et al. (2017), who assimilated measurement data from the CRNS network into the CLM 4.5 model (Oleson et al., 2013). Not only was data assimilation used to update states, but also soil hydraulic parameters were updated using an augmented state vector approach (e.g., Hendricks Franssen and Kinzelbach, 2008). Figure 13 compares the calculated evapotranspiration for a low-quality soil map (assuming homogeneous soil properties) and a high-resolution soil map. Figure 13 also shows that if the homogeneous soil map is used as the basis for the data assimilation experiments, the limited network of nine cosmic ray probes allows updating of the soil hydraulic parameters so that the calculated evapotranspiration is closer to that obtained for the high-resolution soil map.

A second example is indirectly related to hydrology and concerns C fluxes. Post et al. (2017) estimated net ecosystem exchange (NEE) time series using data from four EC towers covering four different plant functional types of the CLM 4.5 model: coniferous forest, grassland, crop, and broadleaf forest. The estimated ecosystem parameters determined for a given plant functional type were applied to all grid cells in the Rur catchment with the same plant functional type. It was found that the estimated ecosystem parameters resulted in leaf area index estimates that were closer to RapidEye data than using default ecosystem parameters. In addition, measured NEE at three additional EC towers was better reproduced, supporting the idea that the estimated ecosystem parameters at single locations can be transferred to the rest of the catchment (Post et al., 2018). Figure 14 shows that NEE is much lower for the run with the estimated ecosystem parameters (areas that act as a C sink are larger than areas that are a C source) than for the run with the default parameters (nearly the complete catchment is a C source).

Summary and Future Perspectives

We provided here an overview of the Rur hydrological observatory, which is part of the TERENO Eifel/Lower Rhine Valley Observatory, accompanied by some highlights of the interdisciplinary and integrated research on the functioning of this catchment. Research in the Rur hydrological observatory focuses on hydrology but also serves as an interdisciplinary platform for various disciplines such as pedology, biogeochemistry, atmospheric sciences, geophysics, and remote sensing. The main research infrastructure in the Rur hydrological observatory has been operational for about a decade and has already provided comprehensive and rich data sets that allow new insights into and interpretations of the functioning of catchments. In addition, a wide range of multi- and interdisciplinary research has been conducted by many researchers from various research institutions. This has led to the development of new observation techniques (e.g., cosmic ray and wireless soil moisture sensing, stable isotope and geophysical measurement techniques) and modeling approaches (e.g., data assimilation methods) to address specific environmental questions.

Presently, more than 1.2 billion data sets from more than 500 measurement stations in the Rur hydrological observatory have already been downloaded from the TERENO data portal. While about 66% of these data sets have been retrieved by internal users within the TERENO consortium, about 34% of the data sets have been downloaded by scientists from all over the world (mostly from academic institutions). Most of the downloaded data sets are related to the soil moisture networks and lysimeter data.

Despite the rich data already available, some information is still lacking for the Rur hydrological observatory. This concerns especially the human influence on hydrological processes, which is important for a more detailed data analysis and modeling. For example, agricultural data, e.g., more precise information on fertilizer application, harvest dates, and yields, is still lacking and notoriously difficult to obtain in a spatially resolved manner. This especially affects the assessment of C and N balances at the catchment scale. Another aspect is missing information on the ecological status of near natural sites, which is important in the framework of ecohydrological studies. Thus, more effort has to be spent on the collection of such data sets for the Rur hydrological observatory, e.g., via cooperation with local agricultural and

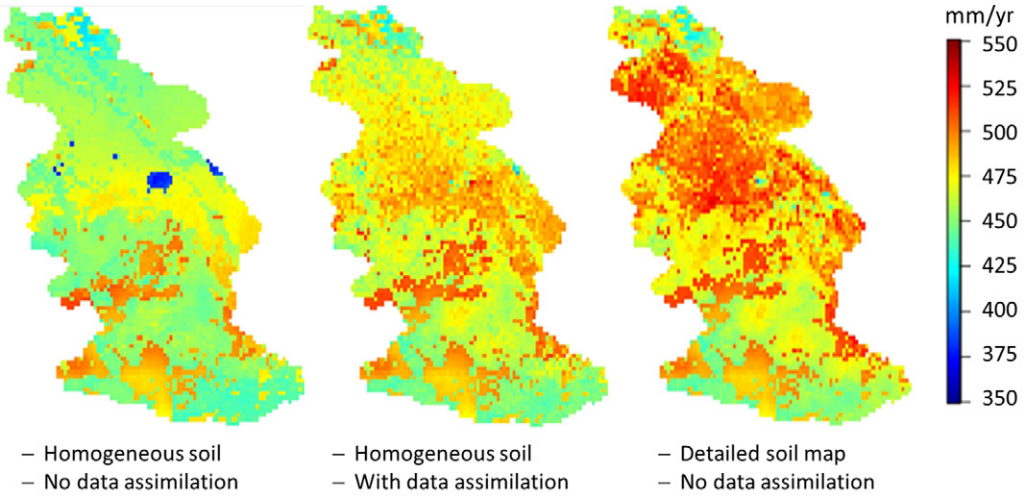

Fig. 13. Different variants of simulated evapotranspiration over the Rur catchment (adapted from Baatz et al., 2017).

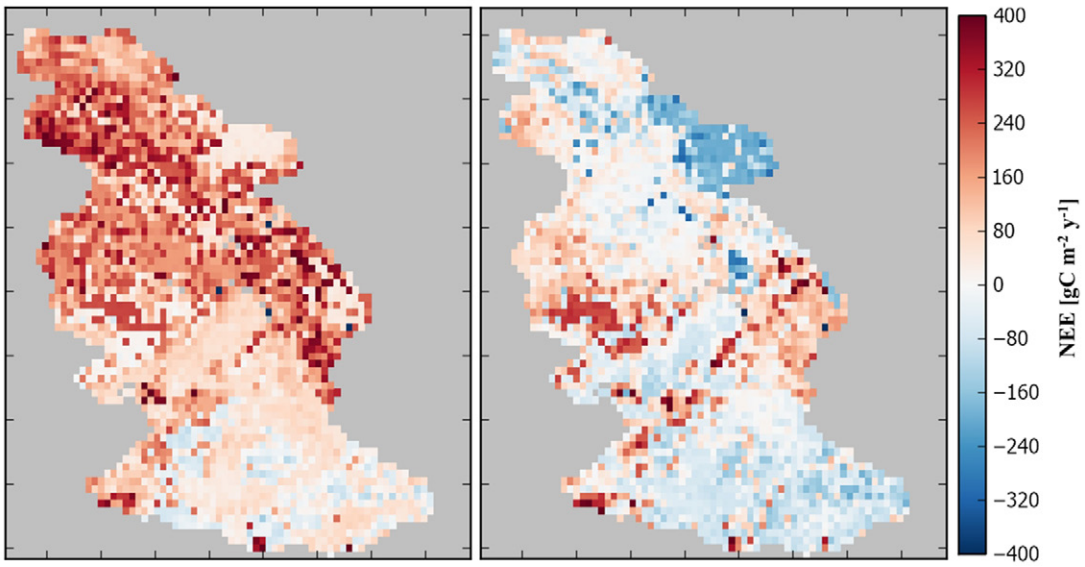

Fig. 14. Annual sum of net ecosystem exchange (NEE) for the Rur catchment (December 2012–November 2013) with default parameters (left) and estimated parameters (right) (adapted from Post et al., 2018).

environmental associations. A good starting point is the close cooperation with the National Park Eifel in the southern part of the Rur catchment.

With our observation and monitoring capabilities set up, we will now focus more on the integration of the data in models to address hydrological predictability at the catchment scale. Data assimilation (i.e., the convolution of observations with a given model state) is the method of choice to achieve this integration because it allows bridging of the gap between observation and prediction of states and fluxes. The large number of available observations will be beneficial to constrain the very large number of model parameters present in distributed models. For instance, prediction by hydrological models is strongly affected by unknown vegetation and soil parameters, which vary strongly in space and even time. Thus, data assimilation should consist of a combined state and parameter estimation approach, e.g., using DART (Anderson et al., 2009) or PDAF (Nerger and Hiller, 2013; Kurtz et al., 2016). Although parameter estimation is sometimes poorly constrained given multiple sources of uncertainty (e.g., uncertain meteorological forcings and model structural issues), it is important to reproduce exchange fluxes like evapotranspiration between terrestrial compartments correctly (Han et al., 2014). The two examples on data assimilation presented here are already very promising starting points in this regard. Future work will also focus on the assimilation of multiple data sets into coupled models across different terrestrial compartments and evaluation of how much predictions can be improved with such an approach. Systematic deviations between model simulations and measurement data can also point to required model improvements and help to detect flaws in the regional model setup or even in the general modeling approach. In addition, multiple models could be used in an ensemble modeling approach to consider uncertainties in process representation across different model types (e.g., one-dimensional soil–vegetation–atmosphere models, hydrological models, and land surface models). The efficient coupling of multi-compartment models and observation data necessitates the use of high-performance computers and flexible and expandable software (e.g., Peckham et al., 2013).

The Rur hydrological observatory is also part of the European Network of Hydrological Observatories (ENOHA, www.enoha.eu) initiative that aims to build up a European data platform for hydrological observatories (Blöschl et al., 2017). Besides making hydrological data available to the research community, we anticipate that ENOHA will also include hydrological models for improved data analysis, for model-driven design of catchment experiments, and to perform hydrological forecasts at the European scale. In addition, data acquired in the Rur hydrological observatory is actively disseminated by feeding it into other databases besides the TERENO data portal, such as the International Soil Moisture Network (ISMN; Dorigo et al., 2011) and the Integrated Carbon Observation System (ICOS) to further ease data usage. Currently, we are working on the generation of download-triggered persistent identifiers to data sets (e.g., doi's) to allow an unambiguous identification and citation of data sets of the Rur hydrological observatory.

Overall, the new insights and novel scientific findings compiled here illustrate that long-term integrated hydrological monitoring within a terrestrial observatory approach as envisioned within the TERENO project is very promising for deepening our understanding of hydrological processes at various scales (i.e., from the field to the catchment). We expect considerable added value of the simultaneous long-term monitoring of a large number of variables across multiple compartments, in particular with respect to previously unresolved links between hydrological and biogeochemical processes.

Data Access

Most data presented in this study are freely available via the TERENO data portal TEODOOR (http://teodoor.icg.kfa-juelich.de/). In addition, three persistent identifiers are associated with the data set of the Rollesbroich test site:

- Climate/Runoff/Water Quality station: http://doi.org/10.5880/TERENO.2016.001
- EC/Climate station Rollesbroich: http://doi.org/10.5880/TERENO.2016.002
- SoilNet Rollesbroich: http://doi.org/10.5880/TERENO.2016.003

The SoilNet data of the Wüstebach catchment is available at https://teodoor.icg.kfa-juelich.de/butt.repository/doi/soilnet.wuestebach/soilnet.wuestebach.wc.2012.8.nc.

Please note that the NetCDF format is used, which is a standard format for data exchange. Free conversion software to convert the NetCDF data format into other data formats is available at http://www.giss.nasa.gov/tools/panoply/.

In addition, EC data from Selhausen (crop), Rollesbroich (grassland), and Wüstebach (forest) will be available at the ICOS data portal with the site codes DE-RuS, DE-RuR, and DE-RuW, respectively (https://www.icos-cp.eu/).

Acknowledgments

We gratefully acknowledge the support of the SFB-TR32 "Pattern in Soil–Vegetation–Atmosphere Systems: Monitoring, Modelling and Data Assimilation" funded by the Deutsche Forschungsgemeinschaft (DFG) and TERENO (Terrestrial Environmental Observatories) funded by the Helmholtz-Gemeinschaft. Further funding for projects contributing to this summary was provided by the German Ministry of Education and Research (BMBF, Grant 01LN1313A). We thank Ferdinand Engels, Rainer Harms, Bernd Schilling, Ansgar Weuthen, Martina Krause, Sirgit Kummer, Werner Küpper, Leander Fürst, Willi Benders, Holger Wissel, Martina Kettler, Nicole Adels, and Daniel Dolfus for supporting the weekly sampling, chemical analysis, and on-going maintenance of the experimental setup.

References

Ali, M., C. Montzka, A. Stadler, G. Menz, F. Thonfeld, and H. Vereecken. 2015. Estimation and validation of RapidEye-based time-series of leaf area index for winter wheat in the Rur catchment (Germany). Remote Sens. 7:2808–2831. doi:10.3390/rs70302808

Altdorff, D., C. von Hebel, N. Borchard, J. van der Kruk, H.R. Bogena, H. Vereecken, and J.A. Huisman. 2017. Potential of catchment-wide soil water content mapping using electromagnetic induction in a forest ecosystem. Environ. Earth Sci. 76:111. doi:10.1007/s12665-016-6361-3

Anderson, J., T. Hoar, K. Raeder, H. Liu, N. Collins, R. Torn, and A. Arellano. 2009. The data assimilation research testbed: A community facility. Bull. Am. Meteorol. Soc. 90:1283–1296. doi:10.1175/2009BAMS2618.1

Andreasen, M., K.H. Jensen, D. Desilets, T. Franz, M. Zreda, H. Bogena, and M.C. Looms. 2017. Status and perspectives of the cosmic-ray neutron method for soil moisture estimation and other environmental science applications. Vadose Zone J. 16(8). doi:10.2136/vzj2017.04.0086

Baatz, R., H. Bogena, H.-J. Hendricks Franssen, J.A. Huisman, C. Montzka, and H. Vereecken. 2015. An empirical vegetation correction for soil water content quantification using cosmic ray probes. Water Resour. Res. 51:2030–2046. doi:10.1002/2014WR016443

Baatz, R., H. Bogena, H.-J. Hendricks Franssen, J.A. Huisman, Q. Wei, C. Montzka, and H. Vereecken. 2014. Calibration of a catchment scale cosmic-ray soil moisture network: A comparison of three different methods. J. Hydrol. 516:231–244. doi:10.1016/j.jhydrol.2014.02.026

Baatz, R., H.-J. Hendricks Franssen, X. Han, T. Hoar, H. Bogena, and H. Vereecken. 2017. Evaluating the value of a network of cosmic-ray probes for improving land surface modeling. Hydrol. Earth Syst. Sci. 21:2509–2530. doi:10.5194/hess-21-2509-2017

Basu, N.B., S.E. Thompson, and P.S.C. Rao. 2011. Hydrologic and biogeochemical functioning of intensively managed catchments: A synthesis of top-down analyses. Water Resour. Res. 47:W00J15. doi:10.1029/2011WR010800

Blöschl, G., H. Bogena, K. Jensen, S. Zacharias, H. Kunstmann, I. Heinrich, et al. 2017. The need for a European data platform for hydrological observatories. In: 19th EGU General Assembly, EGU2017, Proceedings of the Conference, Vienna. 23–28 Apr. 2017. Elsevier Procedia, Amsterdam. p. 8271.

Bogena, H.R., R. Bol, N. Borchard, N. Brüggemann, B. Diekkrüger, C. Drüe, et al. 2015b. A terrestrial observatory approach for the integrated investigation of the effects of deforestation on water, energy, and matter fluxes. Sci. China Earth Sci. 58:61–75. doi:10.1007/s11430-014-4911-7

Bogena, H., J.F. Hake, M. Herbst, R. Kunkel, C. Montzka, T. Pütz, et al. 2005a. MOSYRUR: Water balance analysis in the Rur basin. Schr. Forschungszent. Juelich, Reihe Umwelt/Environ. 52. Forschungszentrum Jülich, Jülich, Germany.

Bogena, H.R., M. Herbst, J.A. Huisman, U. Rosenbaum, A. Weuthen, and H. Vereecken. 2010. Potential of wireless sensor networks for measuring soil water content variability. Vadose Zone J. 9:1002–1013. doi:10.2136/vzj2009.0173

Bogena, H.R., J.A. Huisman, R. Baatz, H.-J. Hendricks Franssen, and H. Vereecken. 2013. Accuracy of the cosmic-ray soil water content probe in humid forested ecosystems: A worst case scenario. Water Resour. Res. 49:5778–5791. doi:10.1002/wrcr.20463

Bogena, H.R., J.A. Huisman, C. Hübner, J. Kusche, F. Jonard, S. Vey, et al. 2015a. Emerging methods for non-invasive sensing of soil moisture dynamics from field to catchment scale: A review. Wiley Interdiscip. Rev.: Water 2:635–647. doi:10.1002/wat2.1097

Bogena, H.R., R. Kunkel, E. Krüger, S. Zacharias, T. Pütz, M. Schwank, et al. 2012. TERENO: Long-term monitoring network for terrestrial research. Hydrol. Wasserbewirtsch. 3:138–143.

Bogena, H., R. Kunkel, T. Schöbel, H.P. Schrey, and F. Wendland. 2005b. Distributed modeling of groundwater recharge at the macroscale. Ecol. Modell. 187:15–26. doi:10.1016/j.ecolmodel.2005.01.023

Bogena, H.R., C. Montzka, H.-J. Hendricks-Franssen, and H. Vereecken. 2018. A blueprint for a distributed terrestrial ecosystem research infrastructure. In: A. Chabbi and H. Loescher, editors, Terrestrial ecosystem research infrastructures: Challenges, new developments and perspectives. CRC Press, Boca Raton, FL. p. 279–302.

Burt, T.P., N.J.K. Howden, F. Worrall, and M.J. Whelan. 2008. Importance of long-term monitoring for detecting environmental change: Lessons from a lowland river in south east England. Biogeosciences 5:1529–1535. doi:10.5194/bg-5-1529-2008

Burt, T.P., G. Pinay, F.E. Matheson, N.E. Haycock, A. Butturini, J.C. Clement, et al. 2002. Water table fluctuations in the riparian zone: Comparative results from a pan-European experiment. J. Hydrol. 265:129–148. doi:10.1016/S0022-1694(02)00102-6

Cai, G., J. Vanderborght, A. Klotzsche, J. van der Kruk, J. Neumann, N. Hermes, and H. Vereecken. 2016. Construction of minirhizotron facilities for investigating root zone processes. Vadose Zone J. 15(9). doi:10.2136/vzj2016.05.0043

Clark, M.P., M.F. Bierkens, L. Samaniego, R.A. Woods, R. Uijlenhoet, K.E. Bennett, et al. 2017. The evolution of process-based hydrologic models: Historical challenges and the collective quest for physical realism. Hydrol. Earth Syst. Sci. 21:3427. doi:10.5194/hess-21-3427-2017

Clark, M.P., Y. Fan, D.M. Lawrence, J.C. Adam, D. Bolster, D.J. Gochis, et al. 2015. Improving the representation of hydrologic processes in earth system models. Water Resour. Res. 51:5929–5956. doi:10.1002/2015WR017096

Colliander, A., T.J. Jackson, R. Bindlish, S. Chan, N. Das, S.B. Kim, et al. 2017. Validation of SMAP surface soil moisture products with core validation sites. Remote Sens. Environ. 191:215–231. doi:10.1016/j.rse.2017.01.021

Cornelissen, T., B. Diekkrüger, and H.R. Bogena. 2014. Significance of scale and lower boundary condition in the 3D simulation of hydrological processes and soil moisture variability in a forested headwater catchment. J. Hydrol. 516:140–153. doi:10.1016/j.jhydrol.2014.01.060

Cornelissen, T., B. Diekkrüger, and H.R. Bogena. 2016. Using high-resolution data to test parameter sensitivity of the distributed hydrological model HydroGeoSphere. Water 8(5):202. doi:10.3390/w8050202

Devaraju, A., S. Jirka, R. Kunkel, and J. Sorg. 2015. Q-SOS: A sensor observation service for accessing quality descriptions of environmental data. ISPRS Int. J. Geoinf. 4:1346–1365. doi:10.3390/ijgi4031346

Devaraju, A., R. Kunkel, H. Bogena, J. Sorg, and H. Vereecken. 2014. A common quality assessment framework for environmental

observation data. In: 14th International Multidisciplinary Scientific Geo-Conference and Expo 2014 (SGEM 2014), Albena, Bulgaria. 17–26 June 2014. Book 2, Vol. 1. Curran Assoc., Red Hook, NY. p. 449–456. doi:10.5593/SGEM2014/B21/S8.057

Diederich, M., A. Ryzhkov, C. Simmer, P. Zhang, and S. Trömel. 2015. Use of specific attenuation for rainfall measurement at X-band radar wavelengths: I. Radar calibration and partial beam blockage estimation. J. Hydrometeorol. 16:487–502. doi:10.1175/JHM-D-14-0066.1

Dorigo, W.A., W. Wagner, R. Hohensinn, S. Hahn, C. Paulik, A. Xaver, et al. 2011. The International Soil Moisture Network: A data hosting facility for global in situ soil moisture measurements. Hydrol. Earth Syst. Sci. 15:1675–1698. doi:10.5194/hess-15-1675-2011

Ehret, U., H.V. Gupta, M. Sivapalan, S.V. Weijs, S.J. Schymanski, G. Blöschl, et al. 2014. Advancing catchment hydrology to deal with predictions under change. Hydrol. Earth Syst. Sci. 18:649–671. doi:10.5194/hess-18-649-2014

Fang, Z., H.R. Bogena, S. Kollet, J. Koch, and H. Vereecken. 2015. Spatio-temporal validation of long-term 3D hydrological simulations of a forested catchment using empirical orthogonal functions and wavelet coherence analysis. J. Hydrol. 529:1754–1767. doi:10.1016/j.jhydrol.2015.08.011

Fang, Z., H.R. Bogena, S. Kollet, J. Koch, and H. Vereecken. 2016. Scale dependent parameterization of soil hydraulic conductivity in the 3D simulation of hydrological processes in a forested headwater catchment. J. Hydrol. 536:365–375. doi:10.1016/j.jhydrol.2016.03.020

Gebler, S., H.-J. Hendricks Franssen, S. Kollet, W. Qu, and H. Vereecken. 2017. High resolution modelling of soil moisture patterns with TerrSysMP: A comparison with sensor network data. J. Hydrol. 547:309–331. doi:10.1016/j.jhydrol.2017.01.048

Gebler, S., H.J. Hendricks Franssen, T. Pütz, H. Post, M. Schmidt, and H. Vereecken. 2015. Actual evapotranspiration and precipitation measured by lysimeters: A comparison with eddy covariance and tipping bucket. Hydrol. Earth Syst. Sci. 19:2145–2161. doi:10.5194/hess-19-2145-2015

Gottselig, N., I. Wiekenkamp, L. Weihermüller, N. Brüggemann, A.E. Berns, H.R. Bogena, et al. 2017. Soil biogeochemistry in a forested headwater catchment: A three dimensional view. J. Environ. Qual. 46:210–218. doi:10.2134/jeq2016.07.0276

Graf, A., H.R. Bogena, C. Drüe, H. Hardelauf, T. Pütz, G. Heinemann, and H. Vereecken. 2014. Spatiotemporal relations between water budget components and soil water content in a forested tributary catchment. Water Resour. Res. 50:4837–4857. doi:10.1002/2013WR014516

Graf, A., J. Werner, M. Langensiepen, A. van de Boer, M. Schmidt, M. Kupisch, and H. Vereecken. 2013. Validation of a minimum microclimate disturbance chamber for net ecosystem flux measurements. Agric. For. Meteorol. 174–175:1–14. doi:10.1016/j.agrformet.2013.02.001

Groh, J., C. Stumpp, A. Lücke, T. Pütz, J. Vanderborght, and H. Vereecken. 2018. Inverse estimation of soil hydraulic and transport properties of layered soils from water stable isotopes and lysimeter data. Vadose Zone J. 17:170168. doi:10.2136/vzj2017.09.0168

Groh, J., J. Vanderborght, T. Pütz, and H. Vereecken. 2016. How to control the lysimeter bottom boundary to investigate the effect of climate change on soil processes? Vadose Zone J. 15(7). doi:10.2136/vzj2015.08.0113

Gueting, N., A. Klotzsche, J. van der Kruk, J. Vanderborght, H. Vereecken, and A. Englert. 2015. Imaging and characterization of facies heterogeneity in an alluvial aquifer using GPR full-waveform inversion and cone penetration tests. J. Hydrol. 524:680–695. doi:10.1016/j.jhydrol.2015.03.030

Gueting, N., T. Vienken, A. Klotzsche, J. van der Kruk, J. Vanderborght, J. Caers, et al. 2017. High resolution aquifer characterization using crosshole GPR full-waveform tomography: Comparison with direct-push and tracer test data. Water Resour. Res. 53:49–72. doi:10.1002/2016WR019498

Han, X.J., H.J. Hendricks-Franssen, X. Li, Y.L. Zhang, C. Montzka, and H. Vereecken. 2013. Joint assimilation of surface temperature and L-band microwave brightness temperature in land data assimilation. Vadose Zone J. 12(3). doi:10.2136/vzj2012.0072

Han, X.J., H.J. Hendricks-Franssen, C. Montzka, and H. Vereecken. 2014. Soil moisture and soil properties estimation in the Community Land Model with synthetic brightness temperature observations. Water Resour. Res. 50:6081–6105. doi:10.1002/2013WR014586

Hasan, S., C. Montzka, C. Rüdiger, M. Ali, H. Bogena, and H. Vereecken. 2014. Soil moisture retrieval from airborne L-band passive microwave using high resolution multispectral data. ISPRS J. Photogramm. Remote Sens. 91:59–71. doi:10.1016/j.isprsjprs.2014.02.005

Hendricks Franssen, H.J., and W. Kinzelbach. 2008. Real-time groundwater flow modelling with the Ensemble Kalman Filter: Joint estimation of states and parameters and the filter inbreeding problem. Water Resour. Res. 44:W09408. doi:10.1029/2007WR006505

Jakobi, J. 2017. Analyzing and modelling of vegetation and soil hydrological processes to enhance the cosmic-ray method. M.A. thesis. Univ. of Bonn, Bonn, Germany.

Katul, G.G., R. Oren, S. Manzoni, C. Higgins, and M.B. Parlange. 2012. Evapotranspiration: A process driving mass transport and energy exchange in the soil–plant–atmosphere–climate system. Rev. Geophys. 50:RG3002. doi:10.1029/2011RG000366

Kerr, Y.H., P. Waldteufel, J.P. Wigneron, S. Delwart, F. Cabot, J. Boutin, et al. 2010. The SMOS mission: New tool for monitoring key elements of the global water cycle. Proc. IEEE 98:666–687. doi:10.1109/JPROC.2010.2043032

Klosterhalfen, A., M. Herbst, L. Weihermüller, A. Graf, M. Schmidt, A. Stadler, et al. 2017. Multi-site calibration and validation of a net ecosystem carbon exchange model for croplands. Ecol. Modell. 363:137–156. doi:10.1016/j.ecolmodel.2017.07.028

Koch, J., S. Stisen, Z. Fang, H.R. Bogena, T. Cornelissen, B. Diekkrüger, and S. Kollet. 2016. Inter-comparison of three distributed hydrological models with respect to the seasonal variability of soil moisture patterns at a small forested catchment. J. Hydrol. 533:234–249. doi:10.1016/j.jhydrol.2015.12.002

Köhli, M., M. Schrön, M. Zreda, U. Schmidt, P. Dietrich, and S. Zacharias. 2015. Footprint characteristics revised for field-scale soil moisture monitoring with cosmic-ray neutrons. Water Resour. Res. 51:5772–5790. doi:10.1002/2015WR017169

Korres, W., T.G. Reichenau, P. Fiener, C.N. Koyama, H.R. Bogena, T. Cornelissen, et al. 2015. Spatio-temporal soil moisture patterns: A meta-analysis using plot to catchment scale data. J. Hydrol. 520:326–341. doi:10.1016/j.jhydrol.2014.11.042

Krause, S., J. Freer, D.M. Hannah, N.J.K. Howden, T. Wagener, and F. Worall. 2013. Catchment similarity concepts for understanding dynamic biogeochemical behavior of river basins. Hydrol. Processes 28:1554–1560. doi:10.1002/hyp.10093

Kupisch, M., A. Stadler, M. Langensiepen, and F. Ewert. 2015. Analysis of spatio-temporal patterns of CO_2 and H_2O fluxes in relation to crop growth under field conditions. Field Crops Res. 176:108–118. doi:10.1016/j.fcr.2015.02.011

Kurtz, W., G. He, S.J. Kollet, R.M. Maxwell, H. Vereecken, and H.J. Hendricks Franssen. 2016. TerrSysMP-PDAF (version 1.0): A modular high performance data assimilation framework for an integrated land surface–subsurface model. Geosci. Model Dev. 9:1341–1360. doi:10.5194/gmd-9-1341-2016

Kurtz, W., A. Lapin, O.S. Schilling, Q. Tang, E. Schiller, T. Braun, et al. 2017. Integrating hydrological modelling, data assimilation and cloud computing for real-time management of water resources. Environ. Modell. Softw. 93:418–435. doi:10.1016/j.envsoft.2017.03.011

Liu, S., M. Herbst, R. Bol, N. Gottselig, T. Pütz, D. Weymann, et al. 2016. The contribution of hydroxylamine content to spatial variability of N_2O formation in soil of a Norway spruce forest. Geochim. Cosmochim. Acta 178:76–86. doi:10.1016/j.gca.2016.01.026

Mauder, M., M. Cuntz, C. Druee, A. Graf, C. Rebmann, H.P. Schmid, et al. 2013. A strategy for quality and uncertainty assessment of long-term eddy-covariance measurements. Agric. For. Meteorol. 169:122–135. doi:10.1016/j.agrformet.2012.09.006

Mohanty, B.P., M.H. Cosh, V. Lakshmi, and C. Montzka. 2017. Soil moisture remote sensing: State-of-the-science. Vadose Zone J. 16(1). doi:10.2136/vzj2016.10.0105

Montzka, C., H.R. Bogena, L. Weihermüller, F. Jonard, C. Bouzinac, J.

Kainulainen, et al. 2013a. Brightness temperature and soil moisture validation at different scales during the SMOS validation campaign in the Rur and Erft catchments, Germany. IEEE Trans. Geosci. Remote Sens. 51:1728–1743. doi:10.1109/TGRS.2012.2206031

Montzka, C., H.R. Bogena, M. Zreda, A. Monerris, R. Morrison, S. Muddu, and H. Vereecken. 2017. Validation of spaceborne and modelled surface soil moisture products with cosmic-ray neutron probes. Remote Sens. 9(2):103. doi:10.3390/rs9020103

Montzka, C., M. Canty, P. Kreins, R. Kunkel, G. Menz, H. Vereecken, and F. Wendland. 2008a. Multispectral remotely sensed data in modelling the annual variability of nitrate concentrations in the leachate. Environ. Modell. Softw. 23:1070–1081. doi:10.1016/j.envsoft.2007.11.010

Montzka, C., M. Canty, R. Kunkel, G. Menz, H. Vereecken, and F. Wendland. 2008b. Modelling the water balance of a mesoscale catchment basin using remotely sensed land cover data. J. Hydrol. 353:322–334. doi:10.1016/j.jhydrol.2008.02.018

Montzka, C., J.P. Grant, H. Moradkhani, H.J. Hendricks-Franssen, L. Weihermuller, M. Drusch, and H. Vereecken. 2013b. Estimation of radiative transfer parameters from L-band passive microwave brightness temperatures using advanced data assimilation. Vadose Zone J. 12(3). doi:10.2136/vzj2012.0040

Montzka, C., T. Jagdhuber, R. Horn, H. Bogena, I. Hajnsek, A. Reigber, and H. Vereecken. 2016. Evaluation of SMAP fusion algorithms with airborne active and passive L-band microwave remote sensing. IEEE Trans. Geosci. Remote Sens. 54:3878–3889. doi:10.1109/TGRS.2016.2529659

Montzka, C., K. Rötzer, H.R. Bogena, and H. Vereecken. 2018. A new soil moisture downscaling approach for SMAP, SMOS and ASCAT by predicting sub-grid variability. Remote Sens. 10(3):427. doi:10.3390/rs10030427

Müller, K., J. Vanderborght, A. Englert, A. Kemna, J. Rings, J.A. Huisman, and H. Vereecken. 2010. Imaging and characterization of solute transport during two tracer tests in a shallow aquifer using electrical resistivity tomography and multilevel groundwater samplers. Water Resour. Res. 46:W03502.

Nerger, L., and W. Hiller. 2013. Software for ensemble-based data assimilation systems: Implementation strategies and scalability. Comput. Geosci. 55:110–118. doi:10.1016/j.cageo.2012.03.026

Ney, P., and A. Graf. 2018. High-resolution vertical profile measurements for carbon dioxide and water vapour concentrations within and above crop canopies. Boundary-Layer Meteorol. 166:449–473. doi:10.1007/s10546-017-0316-4

Oleson, K., D.M. Lawrence, G.B. Bonan, B. Drewniak, M. Huang, C.D. Koven, et al. 2013. Technical description of version 4.5 of the Community Land Model (CLM). Tech. Note NCAR/TN-503+STR. Natl. Ctr. Atmos. Res., Boulder, CO.

Peckham, S.D., E.W.H. Hutton, and B. Norris. 2013. A component-based approach to integrated modeling in the geosciences: The design of CSDMS. Comput. Geosci. 53:3–12. doi:10.1016/j.cageo.2012.04.002

Peters, A., J. Groh, F. Schrader, W. Durner, H. Vereecken, and T. Pütz. 2017. Towards an unbiased filter routine to determine precipitation and evapotranspiration from high precision lysimeter measurements. J. Hydrol. 549:731–740. doi:10.1016/j.jhydrol.2017.04.015

Post, H., H.J. Hendricks Franssen, A. Graf, M. Schmidt, and H. Vereecken. 2015. Uncertainty analysis of eddy covariance CO_2 flux measurements for different EC tower distances using an extended two-tower approach. Biogeosciences 12:1205–1221. doi:10.5194/bg-12-1205-2015

Post, H., H.J. Hendricks Franssen, X.J. Han, R. Baatz, C. Montzka, M. Schmidt, and H. Vereecken. 2018. Evaluation and uncertainty analysis of regional-scale CLM4.5 net carbon flux estimates. Biogeosciences 15:187–208. doi:10.5194/bg-15-187-2018

Post, H., J.A. Vrugt, A. Fox, H. Vereecken, and H.J. Hendricks Franssen. 2017. Estimation of Community Land Model parameters for an improved assessment of net carbon fluxes at European sites. J. Geophys. Res. Biogeosci. 122:661–689. doi:10.1002/2015JG003297

Pütz, T., R. Kiese, U. Wollschläger, J. Groh, H. Rupp, S. Zacharias, et al. 2016. TERENO-SOILCan: A lysimeter-network in Germany observing soil processes and plant diversity influenced by climate change. Environ. Earth Sci. 75:1242. doi:10.1007/s12665-016-6031-5

Qu, W., H.R. Bogena, J.A. Huisman, G. Martinez Garcia, Y. Pachepsky, and H. Vereecken. 2014. Effects of soil hydraulic properties on the spatial variability of soil water content: Evidence from sensor network data and inverse modeling. Vadose Zone J. 13(12). doi:10.2136/vzj2014.07.0099

Qu, W., H.R. Bogena, J.A. Huisman, M. Schmidt, R. Kunkel, A. Weuthen, et al. 2016. The integrated water balance and soil data set of the Rollesbroich hydrological observatory. Earth Syst. Sci. Data 8:517–529. doi:10.5194/essd-8-517-2016

Qu, W., H.R. Bogena, J.A. Huisman, J. Vanderborght, M. Schuh, E. Priesack, and H. Vereecken. 2015. Predicting sub-grid variability of soil water content from basic soil information. Geophys. Res. Lett. 42:789–796. doi:10.1002/2014GL062496

Rabbel, I., H. Bogena, B. Neuwirth, and B. Diekkrüger. 2018. Using sap flow data to parameterize the Feddes water stress model for Norway spruce. Water 10(3):279. doi:10.3390/w10030279

Rahman, M., M. Sulis, and S.J. Kollet. 2016. Evaluating the dual-boundary forcing concept in subsurface–land surface interactions of the hydrological cycle. Hydrol. Processes 30:1563–1573. doi:10.1002/hyp.10702

Reichenau, T.G., W. Korres, C. Montzka, P. Fiener, F. Wilken, A. Stadler, et al. 2016. Spatial heterogeneity of leaf area index (LAI) and its temporal course on arable land: Combining field measurements, remote sensing and simulation in a comprehensive data analysis approach (CDAA). PLoS One 11:e0158451. doi:10.1371/journal.pone.0158451

Robinson, D.A., C.S. Campbell, J.W. Hopmans, B.K. Hornbuckle, S.B. Jones, R. Knight, et al. 2008. Soil moisture measurement for ecological and hydrological watershed-scale observatories: A review. Vadose Zone J. 7:358–389. doi:10.2136/vzj2007.0143

Rosenbaum, U., H.R. Bogena, M. Herbst, J.A. Huisman, T.J. Peterson, A. Weuthen, et al. 2012. Seasonal and event dynamics of spatial soil moisture patterns at the small catchment scale. Water Resour. Res. 48:W10544. doi:10.1029/2011WR011518

Rosenbaum, U., J.A. Huisman, A. Weuthen, H. Vereecken, and H.R. Bogena. 2010. Sensor-to-sensor variability of the ECH_2O EC-5, TE, and 5TE sensors in dielectric liquids. Vadose Zone J. 9:181–186. doi:10.2136/vzj2009.0036

Rötzer, K., C. Montzka, H. Bogena, W. Wagner, R. Kidd, and H. Vereecken. 2014. Catchment scale validation of SMOS and ASCAT soil moisture products using hydrological modelling and temporal stability analysis. J. Hydrol. 519:934–946. doi:10.1016/j.jhydrol.2014.07.065

Rudi, J., R. Pabel, G. Jager, R. Koch, A. Kunoth, and H. Bogena. 2010. Multiscale analysis of hydrologic time series data using the Hilbert–Huang transform. Vadose Zone J. 9:925–942. doi:10.2136/vzj2009.0163

Rudolph, S., J. van der Kruk, C. von Hebel, M. Ali, M. Herbst, C. Montzka, et al. 2015. Linking satellite derived LAI patterns with subsoil heterogeneity using large-scale ground-based electromagnetic induction measurements. Geoderma 241–242:262–271. doi:10.1016/j.geoderma.2014.11.015

Schrön, M., M. Köhli, L. Scheiffele, J. Iwema, H.R. Bogena, L. Lv, et al. 2017. Spatial sensitivity of cosmic-ray neutron sensors applied to improve calibration and validation. Hydrol. Earth Syst. Sci. 21:5009–5030. doi:10.5194/hess-21-5009-2017

Schwaerzel, K., and H.P. Bohl. 2003. An easily installable groundwater lysimeter to determine water balance components and hydraulic properties of peat soils. Hydrol. Earth Syst. Sci. 7:23–32. doi:10.5194/hess-7-23-2003

Siebers, N., S.L. Bauke, F. Tamburini, and W. Amelung. 2018. Short-term impacts of forest clear-cut on P accessibility in soil microaggregates: An oxygen isotope study. Geoderma 315:59–64. doi:10.1016/j.geoderma.2017.11.024

Simmer, C., I. Thiele-Eich, M. Masbou, W. Amelung, H. Bogena, S. Crewell, et al. 2015. Monitoring and modeling the terrestrial system from pores to catchments: The Transregional Collaborative Research Center on patterns in the soil–vegetation–atmosphere system. Bull. Am. Meteorol. Soc. 96:1765–1787. doi:10.1175/BAMS-D-13-00134.1

Stadler, A., S. Rudolph, M. Kupisch, M. Langensiepen, J. van der Kruk, and F. Ewert. 2015. Quantifying the effects of soil variability on crop growth using apparent soil electrical conductivity measurements. Eur. J. Agron. 64:8–20. doi:10.1016/j.eja.2014.12.004

Stockinger, M.P., H.R. Bogena, A. Lücke, B. Diekkrüger, T. Cornelissen, and H. Vereecken. 2016. Tracer sampling frequency influences estimates of young water fraction and streamwater transit time distribution. J. Hydrol. 541:952–964. doi:10.1016/j.jhydrol.2016.08.007

Stockinger, M., H. Bogena, A. Lücke, B. Diekkrüger, M. Weiler, and H. Vereecken. 2014. Seasonal soil moisture patterns control transit time distributions in a forested headwater catchment. Water Resour. Res. 50:5270–5289. doi:10.1002/2013WR014815

Stockinger, M.P., A. Lücke, J.J. McDonnell, B. Diekkrüger, H. Vereecken, and H.R. Bogena. 2015. Interception effects on stable isotope driven streamwater transit time estimates. Geophys. Res. Lett. 42:5299–5308. doi:10.1002/2015GL064622

Stockinger, M.P., A. Lücke, H. Vereecken, and H.R. Bogena. 2017. Accounting for seasonal isotopic patterns of forest canopy intercepted precipitation in streamflow modeling. J. Hydrol. 555:31–40. doi:10.1016/j.jhydrol.2017.10.003

Vereecken, H., J.A. Huisman, H.J. Hendricks Franssen, N. Brüggemann, H.R. Bogena, S. Kollet, et al. 2015. Soil hydrology: Recent methodological advances, challenges, and perspectives. Water Resour. Res. 51:2616–2633. doi:10.1002/2014WR016852

von Hebel, C., S. Rudolph, A. Mester, J.A. Huisman, P. Kumbhar, H. Vereecken, and J. van der Kruk. 2014. Three-dimensional imaging of subsurface structural patterns using quantitative large-scale multi configuration electromagnetic induction data. Water Resour. Res. 50:2732–2748. doi:10.1002/2013WR014864

Vörösmarty, C.J., P.B. McIntyre, M.O. Gessner, D. Dudgeon, A. Prusevich, P. Green, et al. 2010. Global threats to human water security and river biodiversity. Nature 467:555–561. doi:10.1038/nature09440

Wang, J., H.R. Bogena, H. Vereecken, and N. Brüggemann. 2018. Characterization of the effect of redox potential on the emission of greenhouse gases under a varying water regime. Vadose Zone J. 17:170152. doi:10.2136/vzj2017.08.0152

Weigand, S., R. Bol, B. Reichert, A. Graf, I. Wiekenkamp, M. Stockinger, et al. 2017. Spatiotemporal dependency of dissolved organic carbon to nitrate in stream- and groundwater of a humid forested catchment: A wavelet transform coherence analysis. Vadose Zone J. 16(3). doi:10.2136/vzj2016.09.0077

Wiekenkamp, I., J.A. Huisman, H. Bogena, A. Graf, H. Lin, C. Drüe, and H. Vereecken. 2016a. Changes in spatiotemporal patterns of hydrological response after partial deforestation. J. Hydrol. 542:648–661. doi:10.1016/j.jhydrol.2016.09.037

Wiekenkamp, I., J.A. Huisman, H. Bogena, H. Lin, and H. Vereecken. 2016b. Spatial and temporal occurrence of preferential flow in a forested headwater catchment. J. Hydrol. 534:139–149. doi:10.1016/j.jhydrol.2015.12.050

Wu, B., I. Wiekenkamp, Y. Sun, A.S. Fisher, R. Clough, N. Gottselig, et al. 2017. A dataset for three-dimensional distribution of 39 elements including plant nutrients and other metals and metalloids in the soils of a forested headwater catchment. J. Environ. Qual. 46:1510–1518. doi:10.2134/jeq2017.05.0193

Zacharias, S., H. Bogena, L. Samaniego, M. Mauder, R. Fuß, T. Pütz, et al. 2011. A network of terrestrial environmental observatories in Germany. Vadose Zone J. 10:955–973. doi:10.2136/vzj2010.0139

Zhang, H., H.J. Hendricks Franssen, X. Han, J.A. Vrugt, and H. Vereecken. 2017. State and parameter estimation of two land surface models using the Ensemble Kalman Filter and particle filter. Hydrol. Earth Syst. Sci. 21:4927–4958.

Zreda, M., W.J. Shuttleworth, X. Xeng, C. Zweck, D. Desilets, T.E. Franz, et al. 2012. COSMOS: The COsmic-ray Soil Moisture Observing System. Hydrol. Earth Syst. Sci. 16:4079–4099. doi:10.5194/hess-16-4079-2012